

# Online Appendix

## Shocks, Frictions, and Inequality in US Business Cycles

By CHRISTIAN BAYER, BENJAMIN BORN, AND RALPH LUETTICKE \*

### A. Data and parameterization

In this appendix, we first list the data sources and transformations in Appendix A.1 that we employ in order to calibrate the parameters affecting the stationary distribution and to estimate via Bayesian methods those parameters that do not. Appendix A.2 then discusses the re-parameterization of the RANK model steady state. In Appendix A.3, we present the posterior estimates of the structural shock processes. Appendix A.4 contains the variance decompositions of observables not shown in the main text. In Appendix A.5, we provide the credible intervals for all variance decompositions of observables. Appendix A.6 contains historical decompositions of observables and further variables of interest based on the HANK and HANK-X models, and Appendix A.7 provides IRFs to all structural shocks for RANK, HANK, and HANK-X. Finally, Appendix A.8 provides convergence diagnostics for the MCMC chains.

#### A.1. Data: Sources and transformations

##### DATA FOR CALIBRATION

The following list contains the data sources for the average data ratios we target in the calibration of the stationary equilibrium. Unless otherwise noted, all series are available from 1954 to 2019 from the St.Louis FED - FRED database (mnemonics in parentheses).

**Mean illiquid assets.** Fixed assets (K1TTOTL1ES000) over quarterly GDP (excluding net exports; see below), averaged over 1954 – 2019 (U.S. Bureau of Economic Analysis, 2023a).

**Mean government debt.** Gross federal debt held by the public as percent of GDP (FYUGDA188S), averaged over 1954 – 2019 (U.S. Office of Management and Budget and Federal Reserve Bank of St. Louis, 2023).

\* Bayer: University of Bonn, CEPR, CESifo, and IZA (email: christian.bayer@uni-bonn.de); Born: Frankfurt School of Finance & Management, CEPR, CESifo, and ifo Institute (email: b.born@fs.de); Luetticke: University of Tuebingen, CEPR, and CFM (email: ralph.luetticke@uni-tuebingen.de). Codes are available at <https://github.com/BASEforHANK>.

**Average top 10 share of wealth.** Source is the World Inequality Database (2023), averaged over 1954 – 2019.

DATA FOR ESTIMATION

Formally, the vector of observable variables is given by:

$$OBS_t = \begin{bmatrix} \Delta \log(Y_t) \\ \Delta \log(C_t) \\ \Delta \log(I_t) \\ \Delta \log(w_t^F) \\ \log(N_t) \\ \log(R_t^b) \\ \log(\pi_t) \\ \log(T10WShare_t) \\ \log(T10IShare_t) \\ \log(s_t) \\ \log(\tau_t^P) \end{bmatrix} - \begin{bmatrix} \overline{\Delta \log(Y_t)} \\ \overline{\Delta \log(C_t)} \\ \overline{\Delta \log(I_t)} \\ \overline{\Delta \log(w_t^F)} \\ \overline{\log(N_t)} \\ \overline{\log(R_t^b)} \\ \overline{\log(\pi_t)} \\ \overline{\log(T10WShare_t)} \\ \overline{\log(T10IShare_t)} \\ \overline{\log(s_t)} \\ \overline{\log(\tau_t^P)} \end{bmatrix}$$

where  $\Delta$  denotes the temporal difference operator and bars above variables denote time-series averages.

Unless otherwise noted, all series are available at quarterly frequency from 1954Q3 to 2019Q4 from the St.Louis FED - FRED database (mnemonics in parentheses). The data originates from U.S. Bureau of Economic Analysis (2023b); U.S. Bureau of Labor Statistics (2023a,b); Board of Governors of the Federal Reserve System (U.S.); Wu and Xia (2016); Bayer et al. (2019) and U.S. Social Security Administration (2023).

**Output,  $Y_t$ .** Sum of gross private domestic investment (GPDI), personal consumption expenditures for nondurable goods (PCND), durable goods (PCDG), and services (PCESV), and government consumption expenditures and gross investment (GCE) divided by the GDP deflator (GDPDEF) and the civilian noninstitutional population (CNP16OV).

**Consumption,  $C_t$ .** Sum of personal consumption expenditures for nondurable goods (PCND), durable goods (PCDG), and services (PCESV) divided by the GDP deflator (GDPDEF) and the civilian noninstitutional population (CNP16OV).

**Investment,  $I_t$ .** Gross private domestic investment (GPDI) divided by the GDP deflator (GDPDEF) and the civilian noninstitutional population (CNP16OV).

**Real wage,  $w_t^F$ .** Hourly compensation in the nonfarm business sector (COMP-NFB) divided by the GDP deflator (GDPDEF).

**Hours worked**,  $N_t$ . Nonfarm business hours worked (HOANBS) divided by the civilian noninstitutional population (CNP16OV).

**Inflation**,  $\pi_t$ . Computed as the log-difference of the GDP deflator (GDPDEF).

**Nominal interest rate**,  $R_t^b$ . Quarterly average of the effective federal funds rate (FEDFUNDS). From 2009Q1 to 2015Q4, we use the Wu and Xia (2016) shadow federal funds rate.

**Wealth inequality**,  $T10WShare_t$ . p90p100 of US net personal wealth from the World Inequality Database (2023). Available annually 1954 to 2019.

**Income inequality**,  $T10IShare_t$ . p90p100 of US pre-tax national income from the World Inequality Database (2023). Available annually 1954 to 2019.

**Idiosyncratic income risk**,  $s_t$ . We take the estimated time series for the variance of idiosyncratic income from Bayer et al. (2019) who use the Survey of Income and Program Participation. Available from 1983Q1 to 2013Q1.

**Tax progressivity**,  $\tau_t^P$ . We follow Ferriere and Navarro (2023) and construct our measure of tax progressivity using the average and average marginal tax rate:  $P = (AMTR - ATR)/(1 - ATR)$ . For a loglinear tax system, this measure equals the parameter capturing the curvature of the tax function. Available annually 1954 to 2017.

#### DETAILS ON THE CONSTRUCTION OF THE TAX-PROGRESSIVITY MEASURE

We extend the Mertens and Montiel Olea (2018)-calculations of average (ATR) and average marginal tax rates (AMTR) to the years 2013-2017. First, in constructing the ATR series, we obtain total tax liabilities for 1929-2017, from the National Income and Product Accounts (NIPA, U.S. Bureau of Economic Analysis, 2023b), *Table 3.2*. Federal social insurance contributions, which are added to total tax liability, come from NIPA, *Table 3.6*, line 3 and 21. For total income, we take Piketty and Saez (2003)'s income series, which uses a broader income concept based on adjusted gross income, excluding taxable social security and unemployment insurance benefits.

The AMTR is the sum of the average marginal individual income tax rate (AMIITR) and the average marginal payroll tax rate (AMPRT). We follow Ferriere and Navarro (2023) and use Saez (2004)'s income concept.<sup>1</sup> This income concept includes all income items reported on an individual's tax return before deductions and excluding capital gains. Income items include salaries and wages,

<sup>1</sup>For a detailed explanation on the construction of the AMTRs; see Appendix A of Mertens and Montiel Olea (2018). We follow *method 1* for computing the AMIITRs.

small business/farm income, partnership and fiduciary income, dividends, interest, rents, royalties and other small items reported as other income. Realized capital gains are excluded in this measure of income.

To construct the AMTR, we first use several tables from the Statistics of Income (SOI, U.S. Internal Revenue Service, 2023) to construct the discrete distributions of adjusted gross income by income brackets needed for the AMITR. *Table 1.1 All Returns* of the SOI archives contains information on number of returns, adjusted gross income (AGI), and taxable income for different ranges of AGI per return. These ranges define the discretization. Given the distribution is fit for every year and by filing status, *Table 1.2 All Returns: by Marital Status* provides the equivalent table distinguishing by filing status, e.g., married filing jointly or separately, head of household, single, and surviving spouse. *Table 1.3 All Returns: Sources of Income* provides information on how many of these returns reported income from salaries and wages. *Table 1.4 All Returns: Sources of Income, Adjustments, and Tax Items* contains data on taxable income and number of corresponding returns by bracket. *Table 3.3 All Returns: Tax Liability, Tax Credits, and Tax Payments* provides information on how many filed for self-employment and their tax liability. Finally, *Table 3.4* contains the number of returns and adjusted gross income by marginal tax bracket and filing status using.

To construct the Average Marginal Payroll Tax Rate (AMPTR), we collect data from the 2019 Annual Statistical supplement (U.S. Social Security Administration, 2023), *Table 2.A3* (columns 1, 2, 3 and 9), to obtain the taxation of labor and self-employed earnings under the Old Age, Survivors and Disability Insurance (OASDI) and Hospital Insurance (HI) programs. The columns respectively cover the number of covered workers and self employed with maximum earnings as well as total taxable earnings. Their difference allows us to calculate the total taxable earnings of covered workers with earnings *below* the maximum. Information on earnings can be found in *Table 4.B* from the same source.

A.2. RANK calibration

Table A.1 shows the steady-state parameterization of the representative-agent analogue of the HANK model. We adjust the discount factor to match a capital-to-output ratio of 11.44 (quarterly) and the level of the tax rate to match the ratio of government-spending-to-output (0.2). All other parameters are externally chosen and equal to the parameterization of the HANK model.

TABLE A.1—EXTERNAL/CALIBRATED PARAMETERS IN RANK (QUARTERLY FREQUENCY)

Parameter	Value	Description	Target
<b>Households</b>			
$\beta$	0.996	Discount factor	K/Y=11.44
$\xi$	4.000	Relative risk aversion	Kaplan et al. (2018)
$\gamma$	2.000	Inverse of Frisch elasticity	Chetty et al. (2011)
<b>Firms</b>			
$\alpha$	0.680	Share of labor	62% labor income
$\delta_0$	0.018	Depreciation rate	7.0% p.a.
$\bar{\eta}$	11.000	Elasticity of substitution	Price markup 10%
$\bar{\zeta}$	11.000	Elasticity of substitution	Wage markup 10%
<b>Government</b>			
$\bar{\tau}^L$	0.250	Tax rate level	$G/Y = 0.2$
$\bar{\tau}^P$	0.120	Tax progressivity	SoI 1954 - 2019
$\bar{R}^b$	1.000	Nominal rate	Growth $\approx$ interest rate
$\bar{\pi}$	1.000	Inflation	Indexation, w.l.o.g.

## A.3. Estimated structural shock processes

Table A.2 presents prior and posterior distributions of the estimated shock processes. The RANK and HANK version only include seven standard aggregate shocks, while the HANK-X version also includes shocks to income risk and tax progressivity.

TABLE A.2—PRIOR AND POSTERIOR DISTRIBUTIONS OF ESTIMATED SHOCKS AND MEASUREMENT ERRORS

Parameter	Distribution	Prior		Posterior		
		Mean	Std. Dev.	RANK	HANK	HANK-X
Structural Shocks						
$\rho_A$	Beta	0.50	0.20	0.943 (0.915, 0.969)	0.947 (0.918, 0.974)	0.982 (0.960, 0.997)
$\sigma_A$	Inv.-Gamma	0.10	2.00	0.222 (0.178, 0.271)	0.219 (0.167, 0.270)	0.147 (0.118, 0.182)
$\rho_Z$	Beta	0.50	0.20	0.996 (0.994, 0.997)	0.996 (0.994, 0.998)	0.998 (0.997, 0.999)
$\sigma_Z$	Inv.-Gamma	0.10	2.00	0.576 (0.526, 0.629)	0.624 (0.571, 0.682)	0.600 (0.553, 0.652)
$\rho_\Psi$	Beta	0.50	0.20	0.721 (0.667, 0.772)	0.658 (0.600, 0.715)	0.751 (0.692, 0.807)
$\sigma_\Psi$	Inv.-Gamma	0.10	2.00	16.723 (13.019, 20.699)	13.397 (11.042, 16.03)	7.282 (6.623, 8.006)
$\rho_\mu$	Beta	0.50	0.20	0.964 (0.935, 0.989)	0.895 (0.871, 0.917)	0.894 (0.868, 0.917)
$\sigma_\mu$	Inv.-Gamma	0.10	2.00	1.276 (1.116, 1.465)	1.250 (1.099, 1.425)	1.386 (1.208, 1.596)
$\rho_{\mu w}$	Beta	0.50	0.20	0.888 (0.847, 0.925)	0.900 (0.874, 0.922)	0.892 (0.860, 0.918)
$\sigma_{\mu w}$	Inv.-Gamma	0.10	2.00	3.663 (3.105, 4.381)	3.452 (3.002, 3.996)	3.742 (3.170, 4.466)
$\sigma_D$	Inv.-Gamma	0.10	2.00	0.541 (0.457, 0.636)	0.534 (0.444, 0.628)	0.378 (0.326, 0.433)
$\rho_P$	Beta	0.50	0.20	— (—, —)	— (—, —)	0.919 (0.883, 0.950)
$\sigma_P$	Inv.-Gamma	0.10	2.00	— (—, —)	— (—, —)	6.865 (5.839, 8.082)
$\sigma_s$	Gamma	65.00	30.00	— (—, —)	— (—, —)	69.227 (61.367, 78.082)
Measurement Errors						
$\sigma_{I10}^{me}$	Inv.-Gamma	0.05	0.01	— (—, —)	— (—, —)	2.208 (1.868, 2.600)
$\sigma_{W10}^{me}$	Inv.-Gamma	0.05	0.01	— (—, —)	— (—, —)	7.544 (6.412, 8.861)

*Note:* The table displays the estimated shock processes and measurement errors, their priors and posterior means across three model variants: RANK, HANK, and HANK-X. The 90% credible intervals are shown in parentheses. Posteriors are obtained by an MCMC method. The standard deviations have been multiplied by 100 for better readability.

A.4. Variance decompositions of further observables

Figure A.1 shows the variance decomposition of all observables not shown in the main text for the estimated models.



*Note:* Variance decompositions at business cycle frequency of all observables not contained in the main text but used in HANK-X. Income risk is constant in RANK and HANK. Tax progressivity as an exogenous process is omitted.

FIGURE A.1. VARIANCE DECOMPOSITIONS OF FURTHER OBSERVABLES

## A.5. Credible intervals of variance decompositions

Table A.3 shows the credible intervals of all shown variance decomposition of for the RANK, the HANK, and the HANK-X model. The credible intervals are obtained by sampling 1000 times from the posterior.

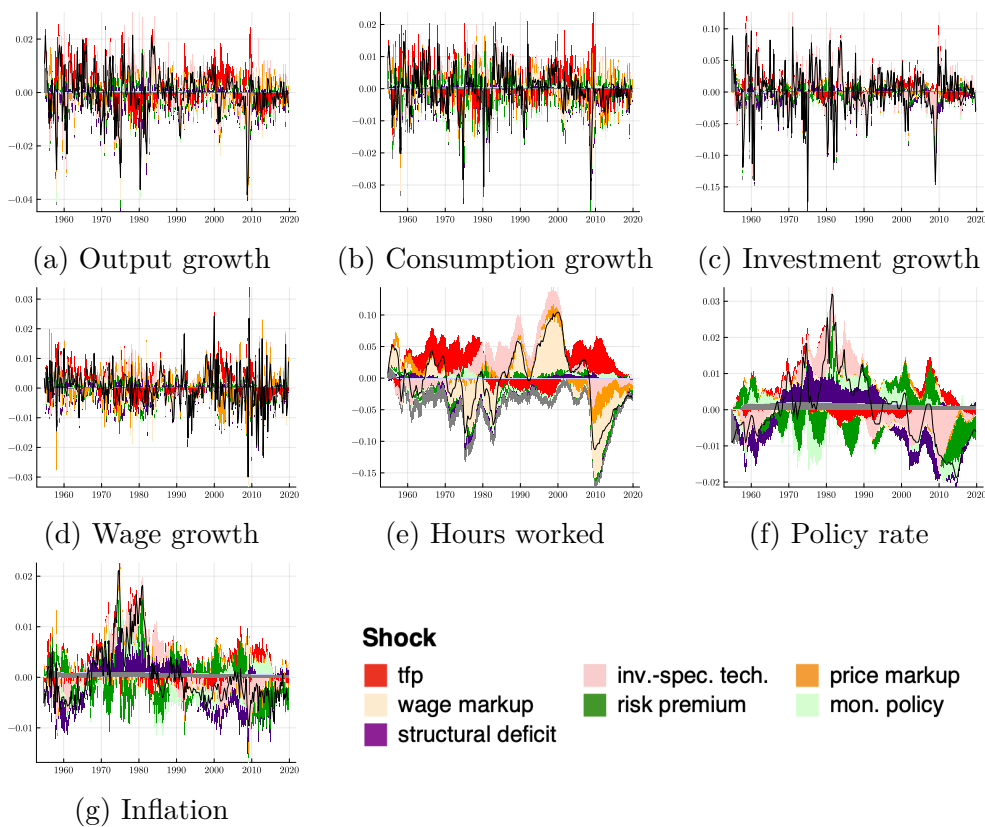
TABLE A.3—VARIANCE DECOMPOSITIONS WITH CREDIBLE INTERVALS

	tfp	inv.-spec. tech.	price markup	wage markup	risk premium	mon. policy	structural deficit	tax progr.	income risk
RANK									
output growth	14.0 (11.2, 16.3)	49.9 (46.4, 54.8)	11.9 (9.5, 15.1)	17.8 (13.2, 18.4)	0.9 (0.5, 2.0)	0.8 (0.5, 1.1)	4.7 (3.3, 5.7)	–	–
consumption growth	27.5 (24.6, 32.3)	7.9 (7.0, 9.2)	14.9 (12.7, 17.6)	38.2 (30.9, 40.0)	7.3 (6.0, 10.3)	3.5 (2.9, 4.9)	0.6 (0.4, 1.1)	–	–
investment growth	0.8 (0.6, 1.0)	95.1 (94.0, 96.2)	1.2 (0.6, 1.8)	0.4 (0.3, 0.6)	0.5 (0.3, 0.7)	0.1 (0.1, 0.2)	1.9 (1.5, 2.1)	–	–
employment	4.2 (3.8, 5.0)	28.7 (25.3, 34.1)	14.2 (11.9, 18.6)	45.7 (39.0, 45.7)	3.4 (2.8, 5.2)	1.5 (1.1, 2.2)	2.3 (1.8, 2.7)	–	–
wage growth	6.5 (4.9, 8.5)	14.8 (13.1, 18.5)	40.4 (38.2, 44.0)	33.9 (29.5, 34.8)	0.4 (0.4, 1.0)	0.1 (0.1, 0.5)	3.8 (2.8, 5.4)	–	–
nominal rate	2.6 (2.3, 3.8)	52.1 (47.6, 57.0)	3.6 (2.5, 5.8)	3.1 (2.2, 4.3)	16.2 (12.3, 20.6)	13.1 (11.1, 14.9)	9.2 (6.1, 12.7)	–	–
inflation	8.5 (7.1, 11.1)	38.0 (32.1, 42.7)	10.5 (7.8, 16.2)	10.6 (8.5, 12.0)	18.2 (14.2, 23.0)	4.3 (3.4, 5.5)	9.7 (6.3, 13.7)	–	–
HANK									
output growth	16.7 (13.9, 19.6)	56.8 (51.8, 62.1)	7.8 (6.1, 9.6)	15.3 (12.3, 18.4)	0.7 (0.3, 1.5)	0.6 (0.5, 0.9)	2.1 (1.4, 3.0)	–	–
consumption growth	30.2 (25.7, 35.3)	22.9 (18.6, 27.5)	14.5 (12.1, 17.1)	23.6 (19.3, 27.5)	5.7 (4.4, 7.5)	2.3 (1.7, 3.1)	0.8 (0.6, 1.5)	–	–
investment growth	1.7 (1.2, 2.3)	93.2 (91.5, 94.6)	0.8 (0.5, 1.2)	0.6 (0.4, 0.9)	1.3 (0.7, 2.0)	0.3 (0.2, 0.4)	2.1 (1.6, 2.7)	–	–
employment	5.2 (4.2, 6.4)	34.4 (28.6, 41.1)	9.0 (7.2, 11.0)	45.7 (39.3, 51.9)	2.8 (1.9, 4.1)	1.1 (0.8, 1.6)	1.7 (1.2, 2.3)	–	–
wage	9.3 (7.2, 11.8)	19.4 (16.3, 24.3)	49.0 (42.9, 53.2)	19.5 (15.3, 23.9)	0.4 (0.2, 1.0)	0.2 (0.1, 0.5)	2.3 (1.5, 3.3)	–	–
nominal rate	2.3 (1.4, 3.4)	42.6 (35.3, 51.2)	1.4 (0.9, 2.2)	2.7 (1.6, 3.9)	21.7 (17.6, 26.3)	17.6 (13.4, 22.0)	11.8 (6.5, 16.3)	–	–
inflation	8.3 (6.2, 10.5)	34.2 (28.3, 41.9)	5.4 (3.7, 7.4)	9.5 (6.9, 11.9)	23.1 (19.0, 27.7)	5.6 (4.3, 7.1)	13.9 (7.9, 19.2)	–	–
HANK-X									
output growth	15.6 (13.0, 18.9)	51.6 (46.9, 56.7)	10.8 (8.8, 13.1)	15.8 (12.6, 18.7)	1.6 (0.9, 2.6)	1.7 (1.3, 2.4)	1.9 (1.2, 2.7)	0.4 (0.3, 0.5)	0.5 (0.4, 0.7)
consumption growth	26.6 (22.1, 31.5)	16.8 (13.9, 20.2)	14.9 (12.4, 17.1)	22.4 (18.0, 25.8)	5.8 (4.7, 7.7)	4.2 (3.4, 5.4)	0.9 (0.7, 1.6)	0.3 (0.2, 0.5)	8.0 (6.4, 10.1)
investment growth	2.1 (1.6, 2.7)	89.7 (87.7, 91.4)	1.9 (1.4, 2.6)	1.3 (1.0, 1.7)	1.7 (1.2, 2.4)	0.7 (0.5, 1.0)	2.4 (1.8, 3.1)	0.0 (0.0, 0.1)	0.1 (0.0, 0.1)
employment	5.5 (4.6, 6.7)	29.7 (25.9, 34.8)	11.6 (9.5, 13.8)	44.5 (38.8, 48.8)	2.9 (2.1, 4.2)	2.5 (2.0, 3.4)	1.6 (1.1, 2.1)	1.1 (0.8, 1.6)	0.6 (0.5, 0.9)
wage	7.7 (6.0, 9.9)	19.4 (16.5, 23.3)	45.8 (40.4, 49.9)	23.0 (18.4, 28.4)	0.9 (0.5, 1.7)	0.9 (0.5, 1.4)	1.4 (0.9, 2.2)	0.6 (0.4, 0.9)	0.3 (0.2, 0.4)
nominal rate	2.4 (1.6, 3.3)	48.4 (40.6, 55.8)	2.5 (1.7, 3.5)	3.7 (2.6, 5.1)	22.0 (17.7, 26.5)	15.0 (11.8, 19.2)	5.2 (2.7, 8.4)	0.2 (0.1, 0.3)	0.7 (0.5, 1.0)
inflation	8.3 (6.4, 10.5)	32.6 (26.6, 38.8)	8.5 (6.2, 11.1)	11.8 (9.0, 14.6)	22.1 (18.2, 26.6)	9.2 (7.5, 11.4)	6.1 (3.3, 9.6)	0.5 (0.3, 0.7)	0.9 (0.6, 1.2)
uncertainty	2.7 (2.1, 3.5)	8.8 (6.8, 11.5)	1.8 (1.3, 2.4)	2.8 (2.1, 3.7)	0.2 (0.1, 0.4)	0.3 (0.2, 0.4)	0.3 (0.2, 0.4)	0.1 (0.0, 0.1)	82.9 (78.4, 86.5)
tax progressivity	0.0 (0.0, 0.0)	0.0 (0.0, 0.0)	100.0 (100.0, 100.0)	0.0 (0.0, 0.0)					
T10 wealth share	1.6 (1.1, 2.2)	47.1 (39.2, 54.5)	37.4 (31.0, 43.0)	2.4 (1.2, 4.1)	4.7 (3.3, 7.8)	2.2 (1.7, 2.9)	1.3 (0.8, 1.8)	3.0 (1.9, 4.3)	0.3 (0.2, 0.5)
T10 income share	6.9 (5.8, 8.5)	35.1 (28.3, 42.8)	32.2 (26.7, 36.9)	19.1 (14.8, 23.9)	2.5 (1.6, 4.1)	0.8 (0.6, 1.2)	1.5 (1.2, 2.0)	0.4 (0.3, 0.5)	1.6 (1.2, 2.1)

*Note:* The table displays variance decompositions at business cycle frequencies and their (5,95)-credible intervals for all observables and shocks in the RANK, HANK, and HANK-X models. The credible intervals are obtained by sampling 1000 times from the posterior.

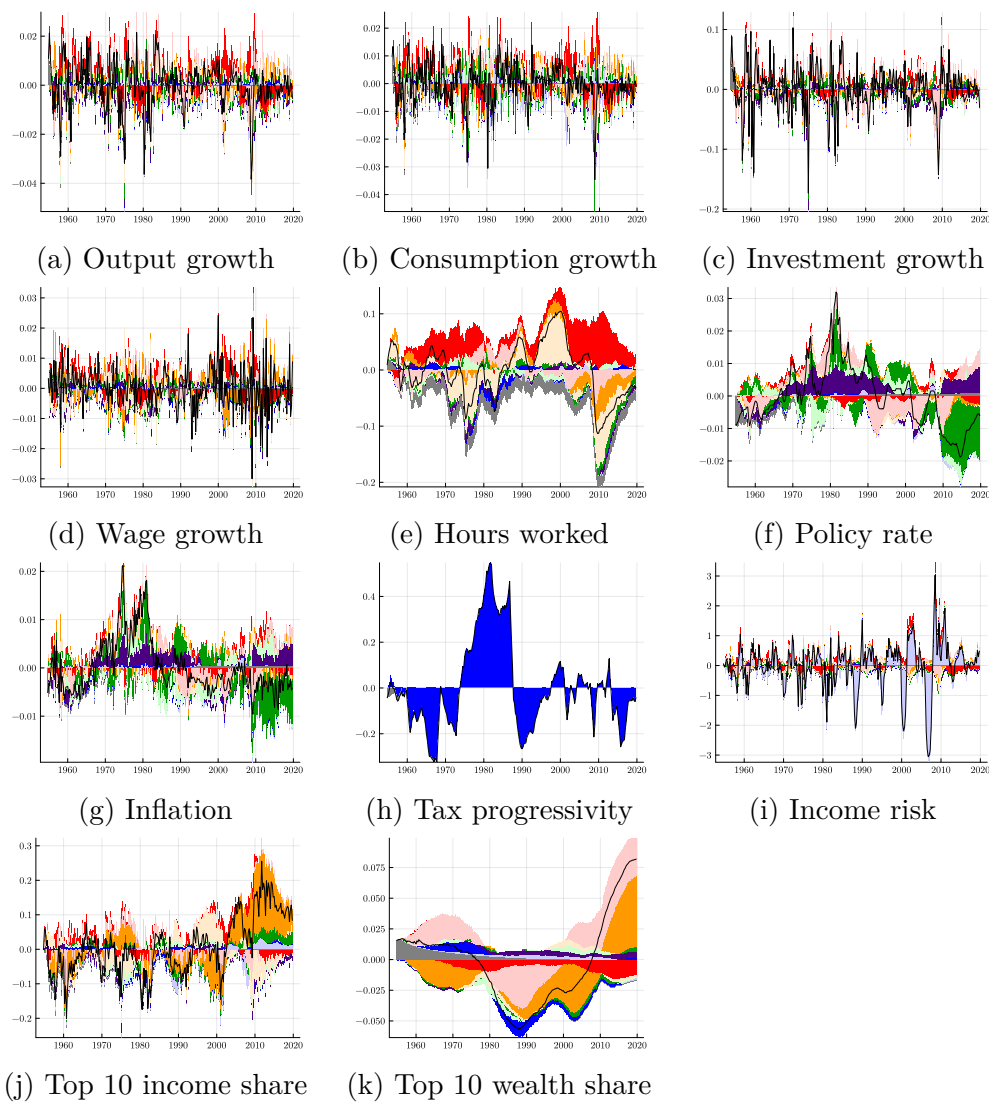
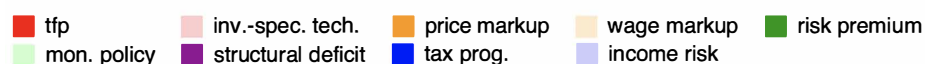
A.6. Historical decompositions of further observables

Figure A.2 shows the historical decomposition of all observables for the estimation of the HANK model and Figures A.3 for the HANK-X model. Figure A.4 shows the historical decomposition of non-observed variables target markups, profits, and the Top 1 percent share of income in the HANK-X model.



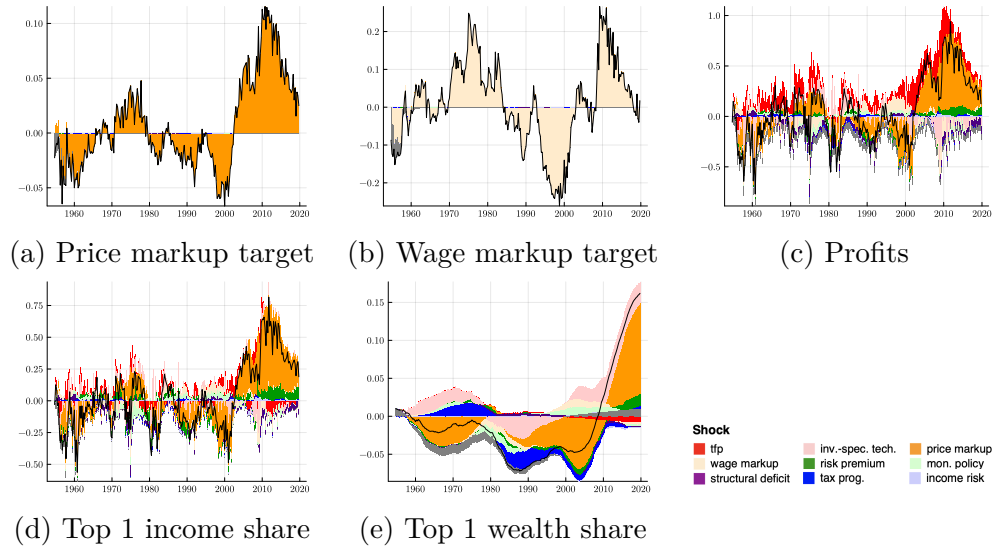
Note: Historical decompositions of all observables in HANK. Y-axis: Percent deviation from mean.

FIGURE A.2. HISTORICAL DECOMPOSITIONS OF OBSERVABLES IN HANK

**Shock**

*Note:* Historical decompositions of all observables in HANK-X. Y-axis: Percent deviation from mean.

FIGURE A.3. HISTORICAL DECOMPOSITIONS OF OBSERVABLES IN HANK-X

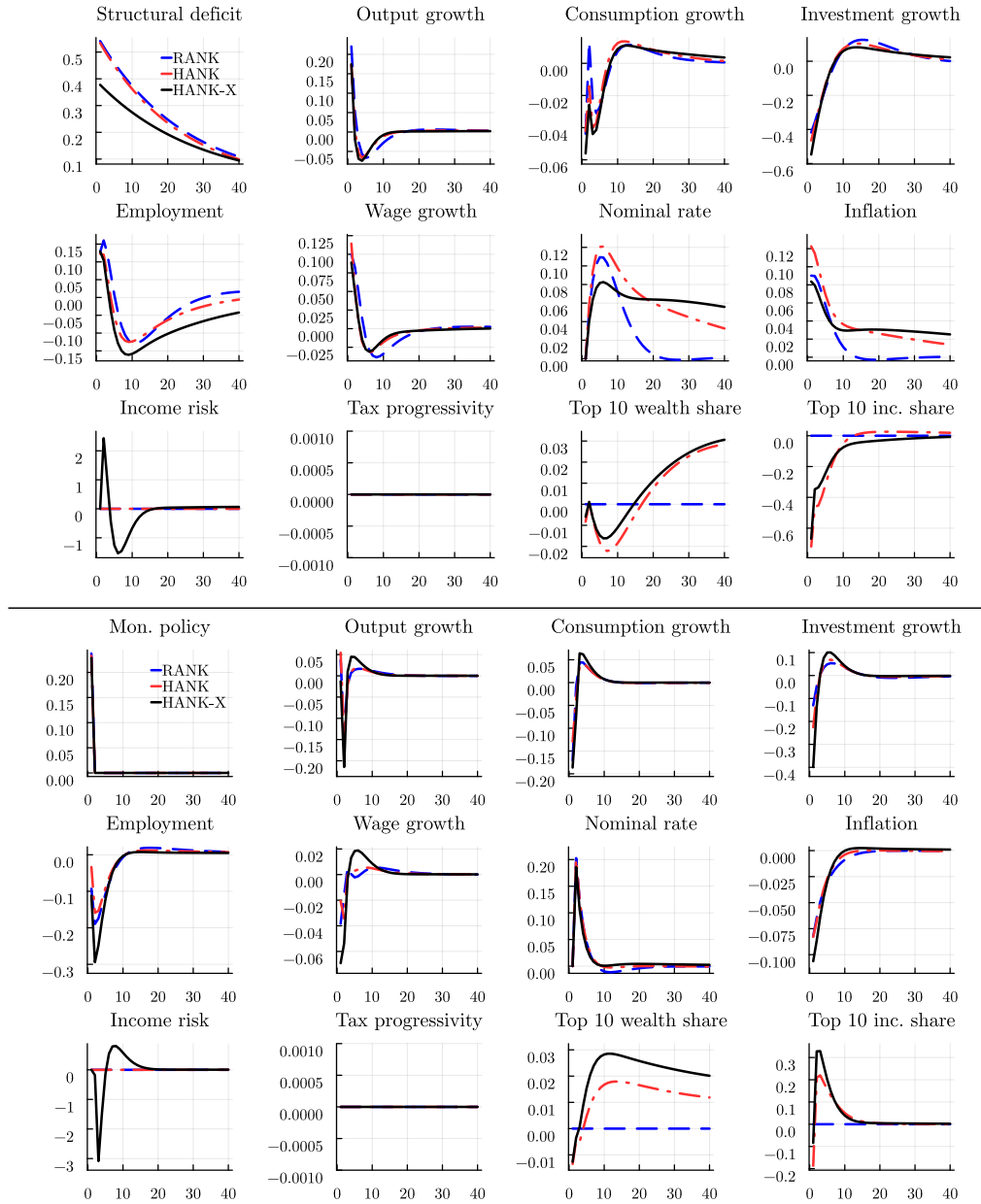


*Note:* Historical decompositions of further unobserved variables in HANK-X. Y-axis: Percent deviation from mean.

FIGURE A.4. HISTORICAL DECOMPOSITIONS OF FURTHER VARIABLES IN HANK-X

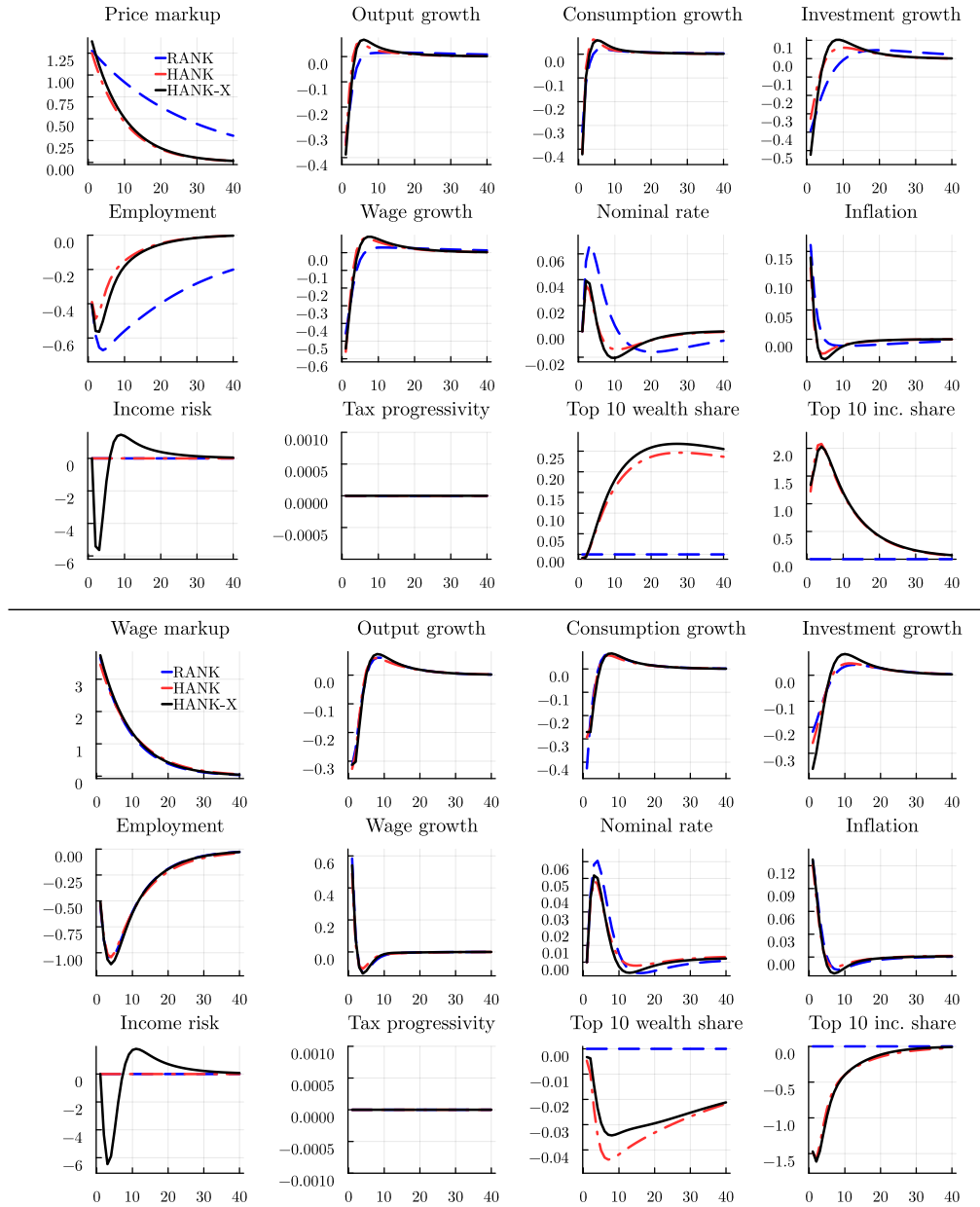
### A.7. Impulse Responses

Figures A.5 – A.9 plot the impulse response functions for the estimated RANK, HANK, and HANK-X model. The first panel on the top left corner of each figure shows the shock and the remaining panels show the responses of all potential observables.



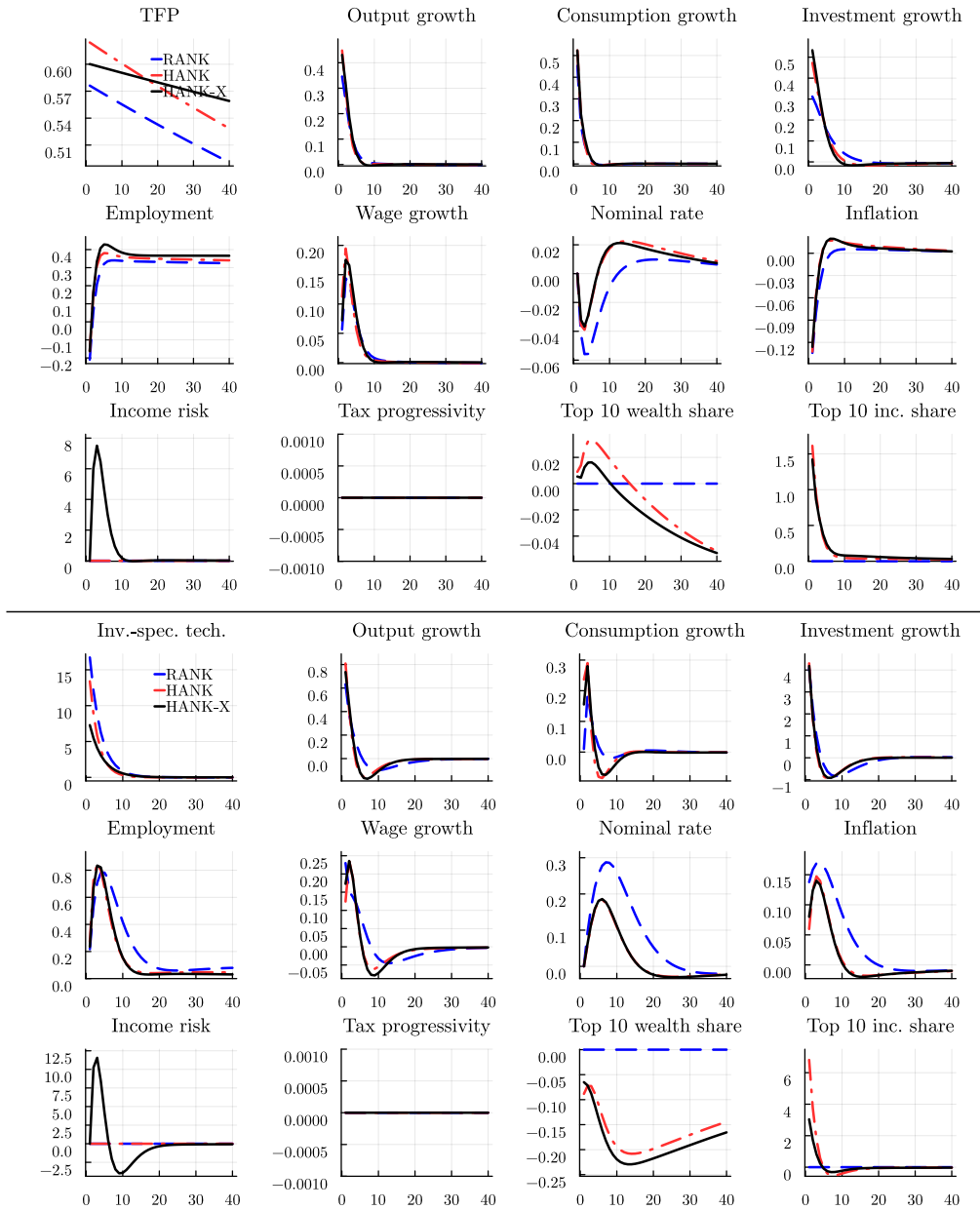
*Note:* Top: IRF to a structural deficit shock. Bottom: IRF to a monetary policy shock. Blue-dashed line: RANK; red dashed-dotted line: HANK; black solid line: HANK-X. Y-axis: Percentage points for the nominal rate and inflation, otherwise percent.

FIGURE A.5. IRFS TO STRUCTURAL DEFICIT AND MONETARY POLICY SHOCKS



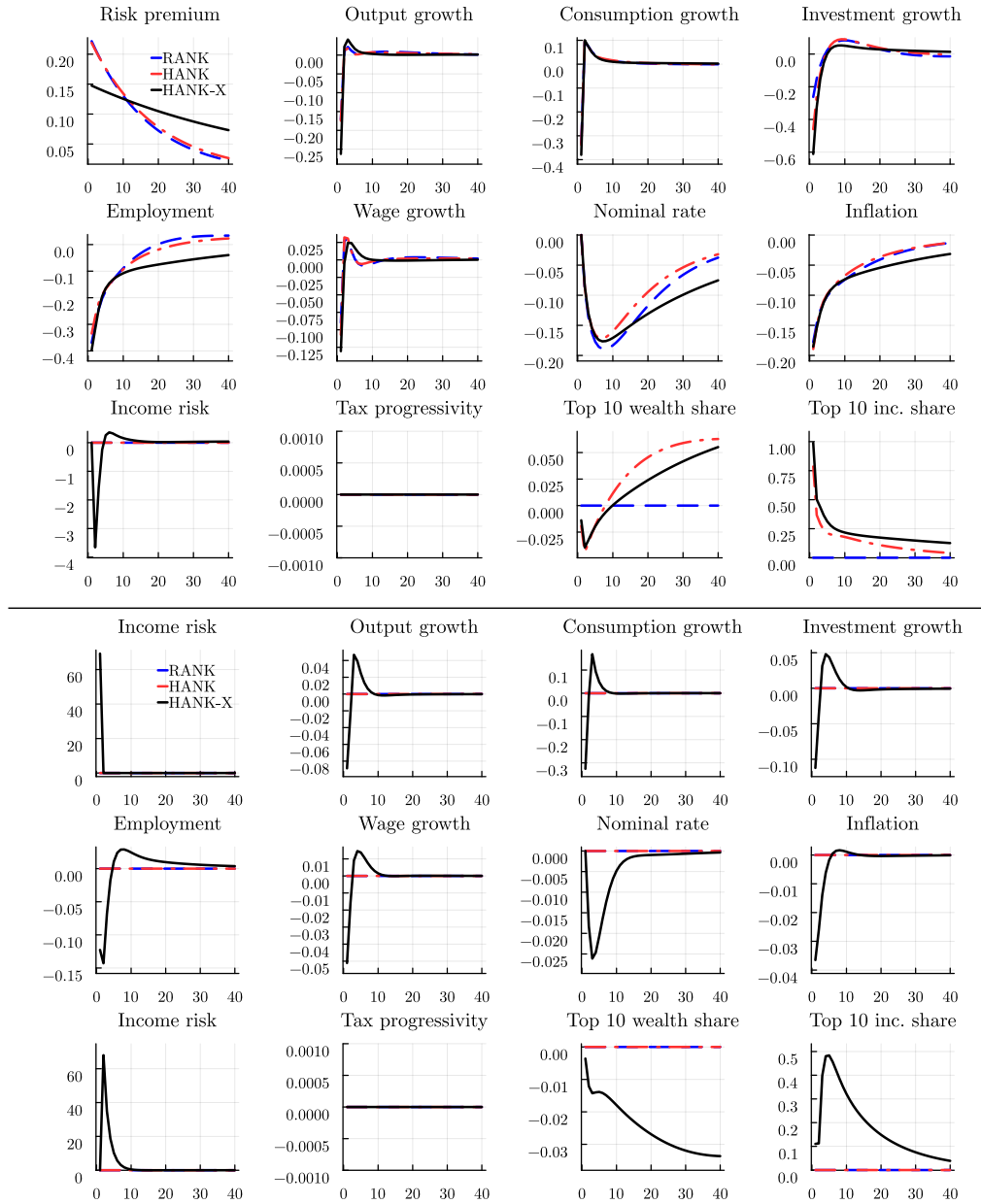
Note: Top: IRF to a price-markup shock. Bottom: IRF to a wage-markup shock. Blue-dashed line: RANK; red dashed-dotted line: HANK; black solid line: HANK-X. Y-axis: Percentage points for the nominal rate and inflation, otherwise percent.

FIGURE A.6. IRFS TO MARKUP SHOCKS



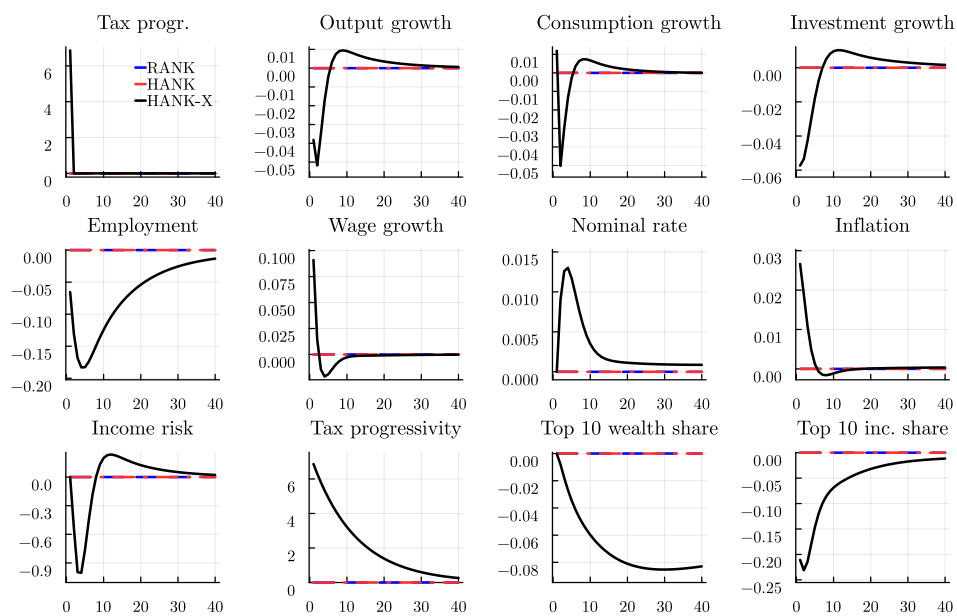
*Note:* Top: IRF to a TFP shock. Bottom: IRF to an MEI shock. Blue-dashed line: RANK; red dashed-dotted line: HANK; black solid line: HANK-X. Y-axis: Percentage points for the nominal rate and inflation, otherwise percent.

FIGURE A.7. IRFs TO TECHNOLOGY SHOCKS



Note: Top: IRF to a risk premium shock. Bottom: IRF to an income risk shock. Blue-dashed line: RANK; red dashed-dotted line: HANK; black solid line: HANK-X. Y-axis: Percentage points for the nominal rate and inflation, otherwise percent.

FIGURE A.8. IRFS TO RISK PREMIUM AND INCOME RISK SHOCKS



*Note:* IRF to a tax progressivity shock. Blue-dashed line: RANK; red dashed-dotted line: HANK; black solid line: HANK-X. Y-axis: Percentage points for the nominal rate and inflation, otherwise percent.

FIGURE A.9. IRFS TO A TAX PROGRESSIVITY SHOCK

*A.8. MCMC diagnostics*

We estimate each model using a single RWMH chain after an extensive mode search. After burn-in, 400,000 draws from the posterior distribution are used to compute the posterior statistics. The acceptance rates across chains are between 20% and 30%. Here, we provide Geweke (1992) convergence statistics for individual parameters of the RANK, HANK, and HANK-X models as well as traceplots for HANK and HANK-X. Geweke (1992) tests the equality of means of the first 10% of draws and the last 50% of draws (after burn-in). If the samples are drawn from the stationary distribution of the chain, the two means are equal and Geweke's statistic has an asymptotically standard normal distribution. Table A.4 reports the Geweke z-score statistic and the p-value for each parameter. Taking the evidence from Geweke (1992) and the traceplot graphs together, we conclude that our chains have converged. No individual Geweke test rejects at the one percent level and only a small number reject at the five percent level, which can be expected from the multiple-testing nature of the exercise.

TABLE A.4—GEWEKE (1992) CONVERGENCE DIAGNOSTICS

Parameter	RANK		HANK		HANK-X	
	z-stat	p-value	z-stat	p-value	z-stat	p-value
$\delta_s$	-0.013	0.989	-2.101	0.036	1.340	0.180
$\phi$	-0.256	0.798	-2.241	0.025	-0.622	0.534
$\kappa$	-0.968	0.333	0.712	0.476	-0.374	0.708
$\kappa_w$	1.149	0.251	0.769	0.442	-0.819	0.413
$\iota^\Pi$	—	—	0.580	0.562	-0.152	0.879
$\rho_A$	-0.551	0.582	0.835	0.404	-0.875	0.382
$\sigma_A$	0.594	0.552	-0.873	0.383	1.149	0.251
$\rho_Z$	0.600	0.549	0.156	0.876	-0.343	0.732
$\sigma_Z$	-0.50	0.617	0.065	0.948	2.193	0.028
$\rho_\Psi$	-0.062	0.950	-2.144	0.032	0.896	0.370
$\sigma_\Psi$	-0.295	0.768	-0.701	0.483	-0.515	0.606
$\rho_\mu$	-1.178	0.239	0.086	0.932	-1.444	0.149
$\sigma_\mu$	0.363	0.716	-0.38	0.704	1.479	0.139
$\rho_{\mu w}$	1.355	0.175	0.593	0.553	-0.172	0.863
$\sigma_{\mu w}$	-1.375	0.169	0.065	0.948	0.400	0.689
$\rho_s$	—	—	—	—	1.458	0.145
$\sigma_s$	—	—	—	—	-0.483	0.629
$\Sigma_y$	—	—	—	—	0.221	0.825
$\rho_R$	-0.327	0.744	0.214	0.831	-0.284	0.777
$\sigma_R$	-0.272	0.786	-0.609	0.542	0.857	0.391
$\theta_\pi$	1.215	0.224	1.024	0.306	-0.392	0.695
$\theta_Y$	-0.395	0.693	0.985	0.324	0.598	0.550
$\gamma_B$	-0.497	0.619	-0.236	0.813	-0.223	0.823
$\gamma_\pi$	0.601	0.548	1.862	0.063	0.360	0.719
$\gamma_Y$	-0.55	0.582	0.617	0.537	-1.463	0.143
$\rho_D$	-0.155	0.877	0.607	0.544	1.774	0.076
$\sigma_D$	-0.81	0.418	-0.771	0.440	-0.42	0.674
$\rho_\tau$	0.930	0.352	-0.289	0.773	-0.574	0.566
$\gamma_B^\tau$	1.263	0.206	-0.216	0.829	0.131	0.896
$\gamma_Y^\tau$	1.048	0.295	1.827	0.068	-0.513	0.608
$\rho_P$	—	—	—	—	-1.407	0.159
$\sigma_P$	—	—	—	—	-0.734	0.463
$\sigma_{W10}^{me}$	—	—	—	—	0.197	0.844
$\sigma_{I10}^{me}$	—	—	—	—	0.011	0.991

Note: Note: Geweke (1992) equality of means test of the first 10% vs. the last 50% of draws. Failure to reject the null of equal means indicates convergence.

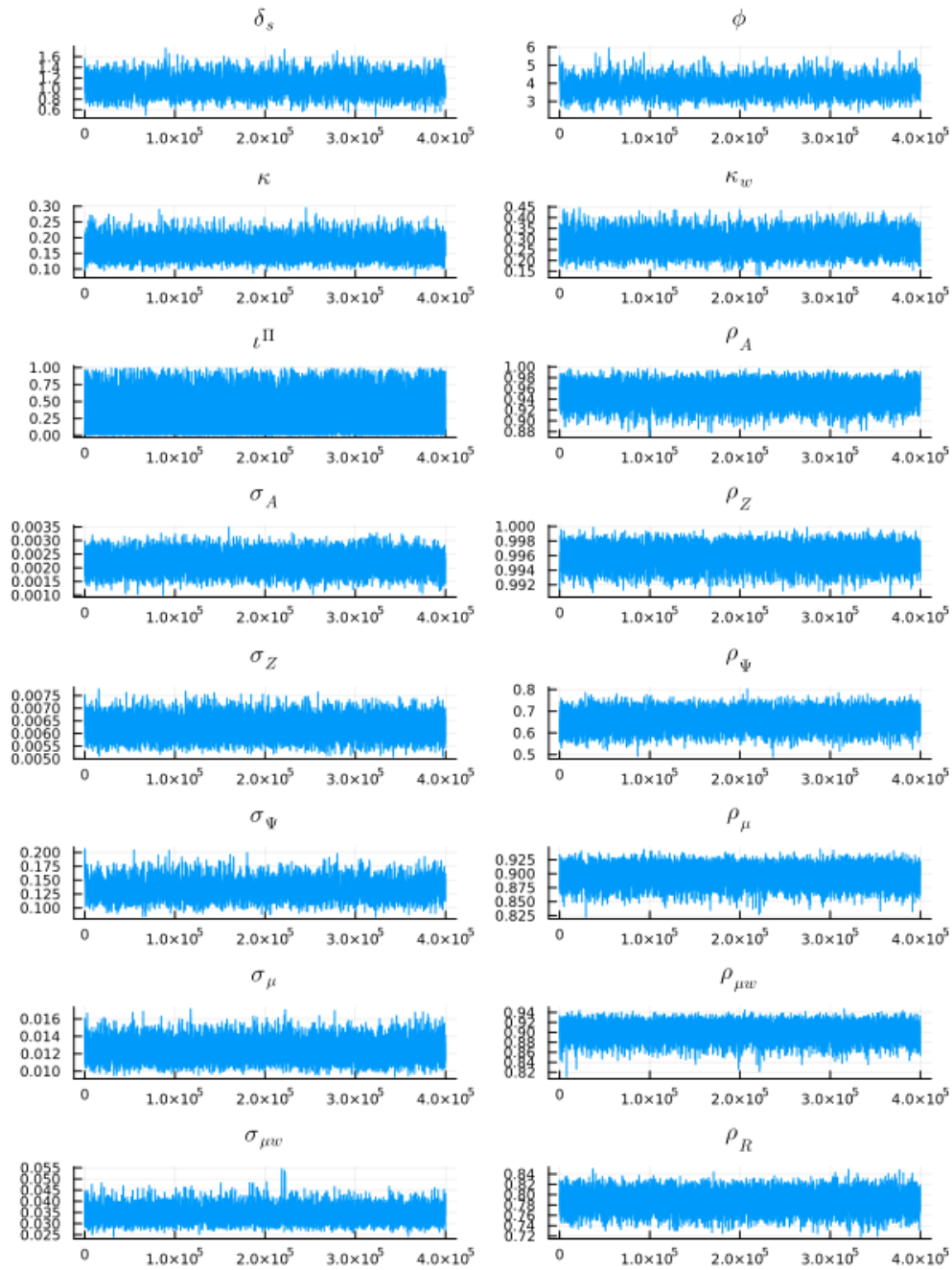


FIGURE A.10. MCMC DRAWS OF HANK MODEL

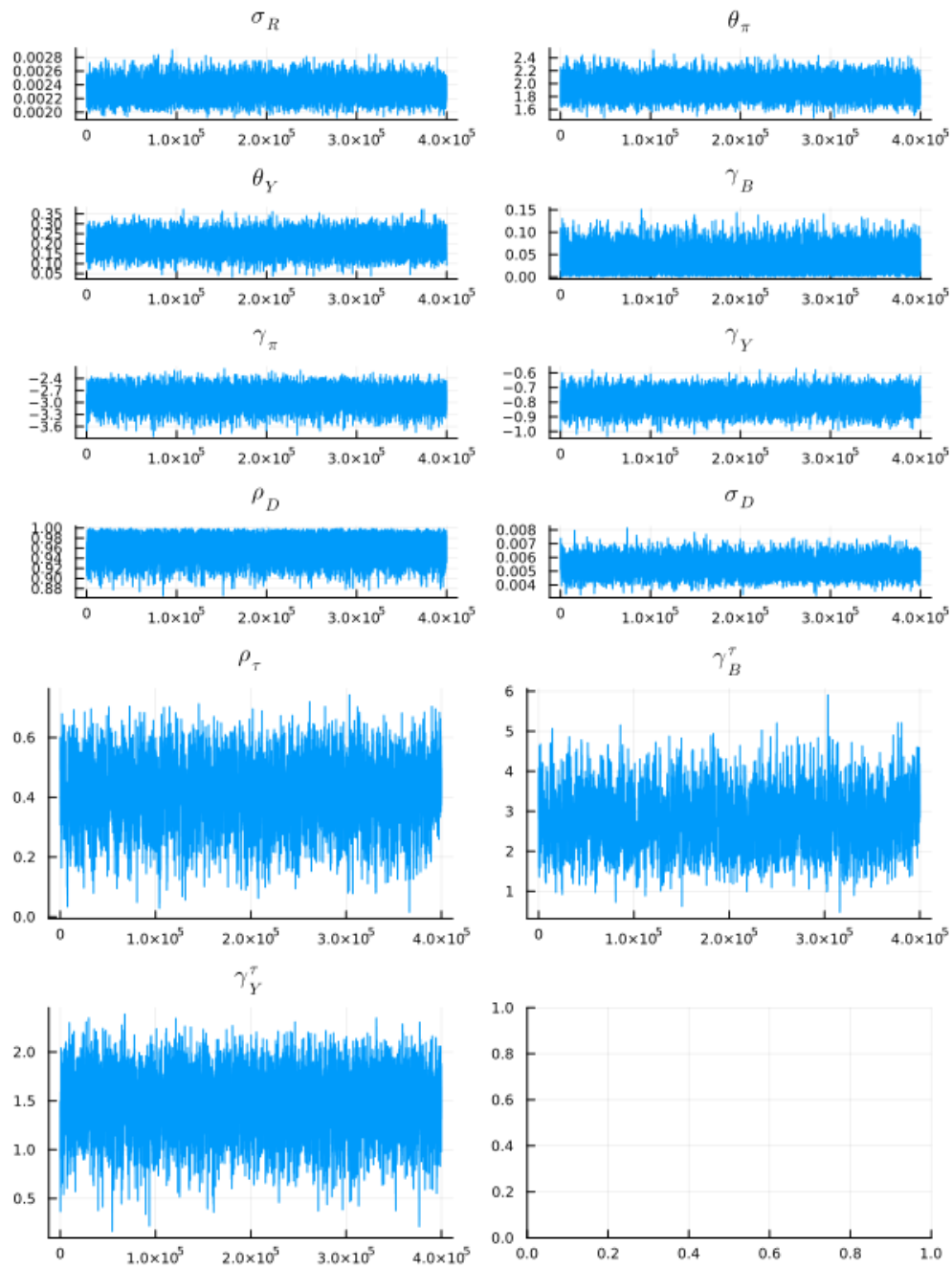


FIGURE A.11. MCMC DRAWS OF HANK MODEL

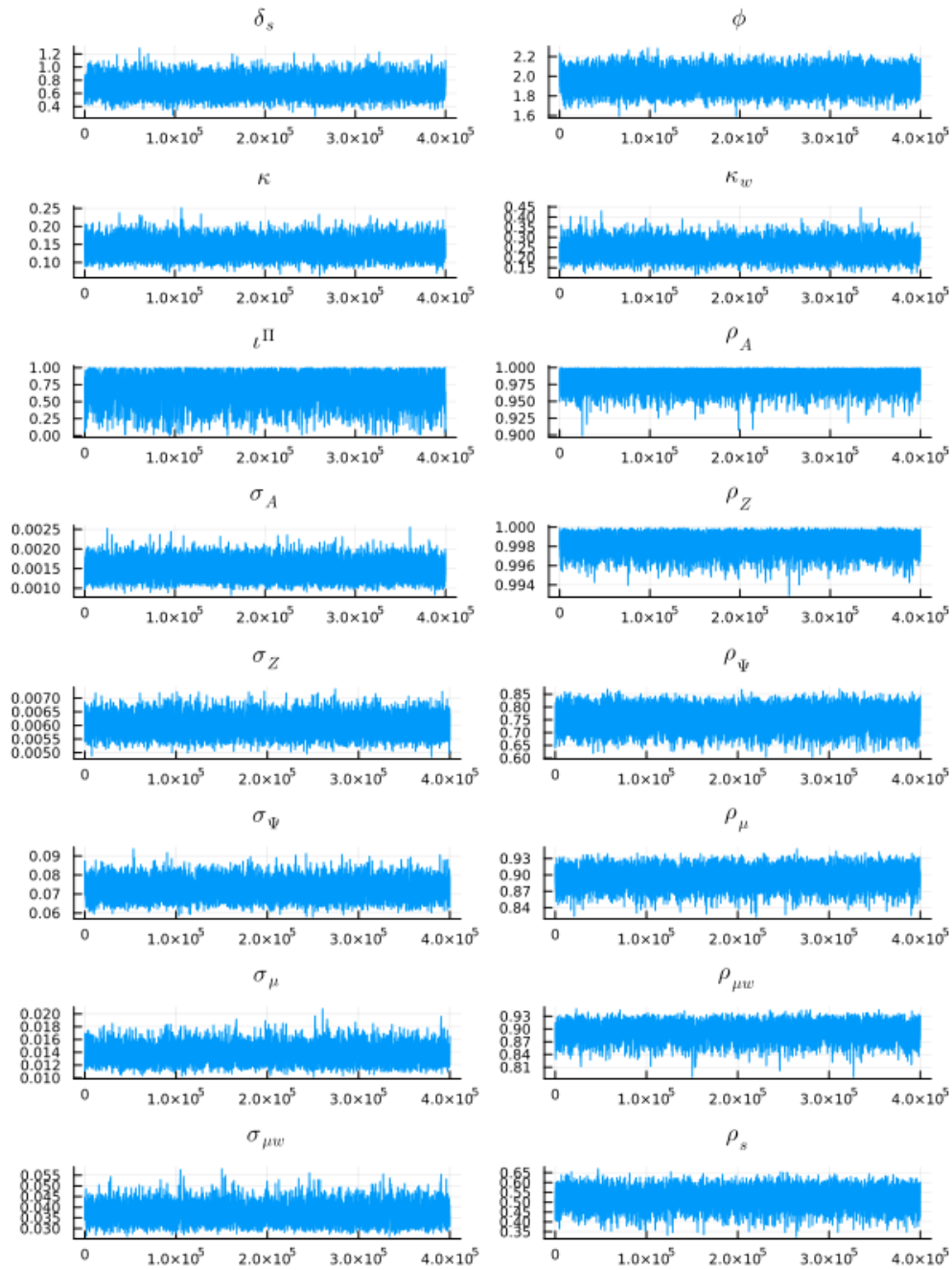


FIGURE A.12. MCMC DRAWS OF HANK-X MODEL

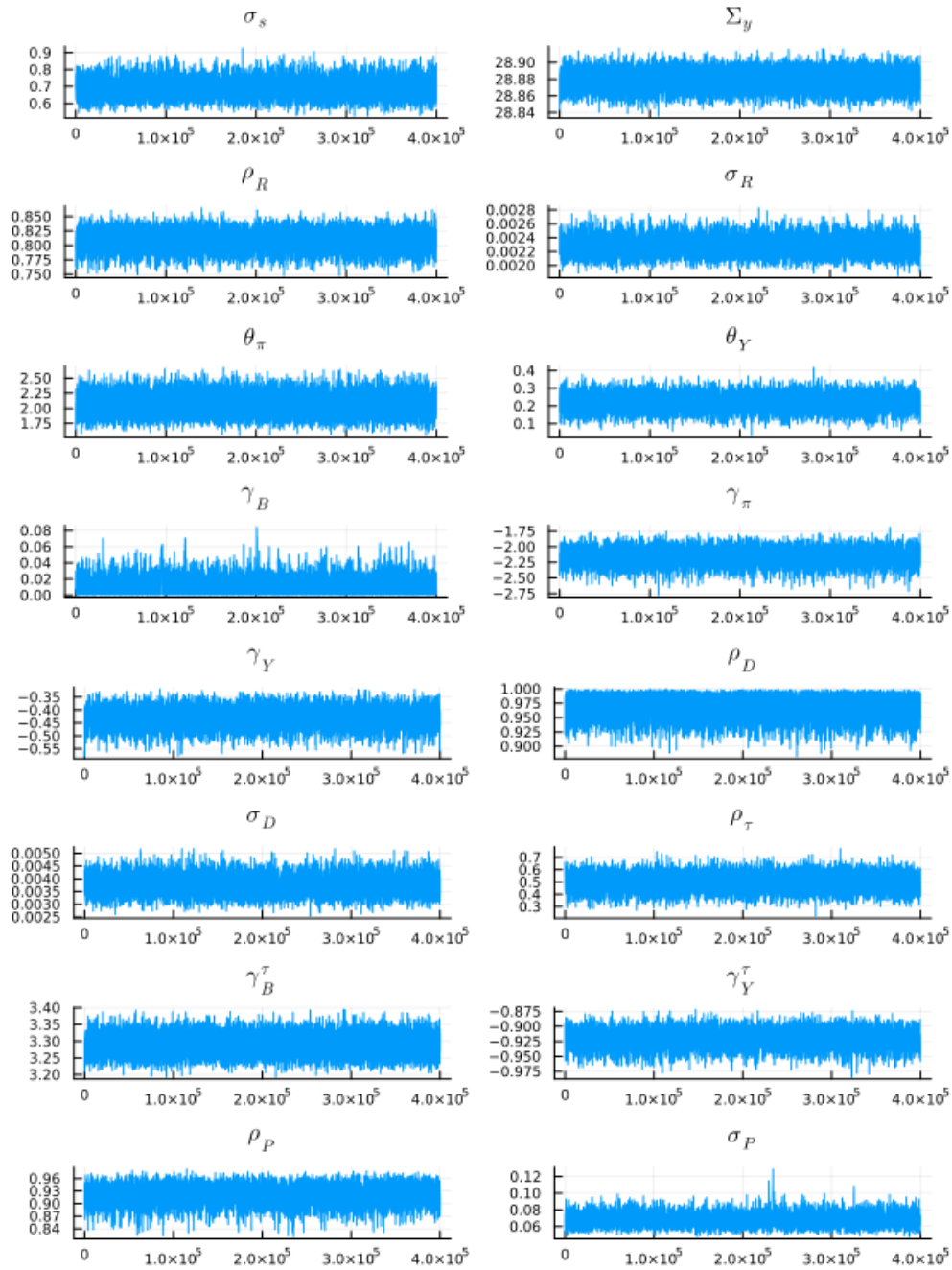


FIGURE A.13. MCMC DRAWS OF HANK-X MODEL

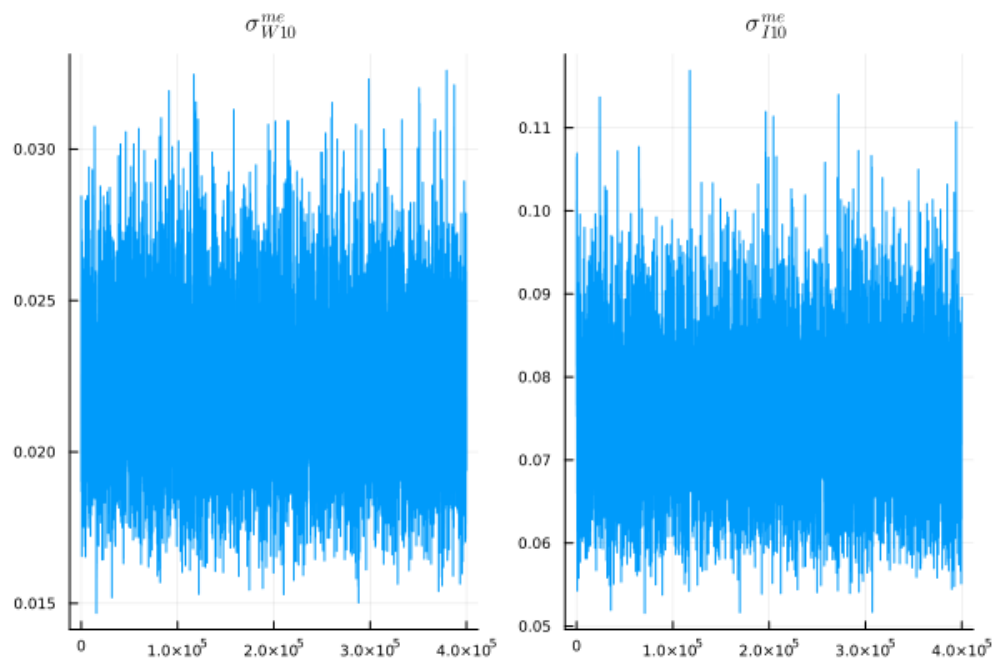


FIGURE A.14. MCMC DRAWS OF HANK-X MODEL

## B. Robustness to alternative specifications

We estimate five variants of our model to understand the effect of potentially important data and modeling choices: 1) sample 1983-2019, 2) risk aversion (2 instead of 4), 3) paying out union profits proportional to idiosyncratic productivity (no wage compression), 4) systematic response of tax progressivity to income inequality, 5) King, Plosser and Rebelo (1988) preferences instead of Greenwood, Hercowitz and Huffman (1988).

Appendix B.1 provides more details on each variant. Appendix B.2 contains the estimated parameters, Appendix B.3 the variance decompositions for all variants, and Appendix B.4 the historical decomposition of income and wealth inequality for the variants with risk aversion 2 and KPR preferences.

### B.1. Description of variants

Below we quickly describe the recalibration of the steady state for variants 2) risk aversion, 3) union profits, and 5) KPR preferences. The other two variants, 1) sample split and 4) fiscal response to inequality, do not require a recalibration of the steady state. The sample split estimation is run using the same model and calibration as in the baseline. Allowing for a feedback coefficient of tax progressivity to the top 10 income share only affects the aggregate model part.

#### RISK AVERSION 2

Changing the coefficient of relative risk aversion to 2 (instead of 4) requires a recalibration of the steady state to match the same targets as listed in Table 1. In particular, we adjust the discount factor, the asset market participation frequency, the fraction of entrepreneurs, and the borrowing penalty. The re-calibration yields  $\beta = 0.992$ ,  $\lambda = 4.5\%$ ,  $\zeta = 1/3750$ , and  $\bar{R} = 2.18\%$ .

#### PROPORTIONAL UNION PROFITS

Paying out union profits proportional to idiosyncratic productivity (instead of lump sum) affects the steady-state distribution of income and requires a recalibration. Again, we adjust the discount factor, the asset market participation frequency, the fraction of entrepreneurs, and the borrowing penalty. The recalibration yields  $\beta = 0.982$ ,  $\lambda = 7.0\%$ ,  $\zeta = 1/7500$ , and  $\bar{R} = 1.35\%$ .

#### FISCAL RESPONSE TO INEQUALITY

We change the policy rule for the tax progressivity parameter,  $\tau_t^P$ , in HANK-X to the following:

$$(B.1) \quad \frac{\tau_t^P}{\bar{\tau}^P} = \left( \frac{\tau_{t-1}^P}{\bar{\tau}^P} \right)^{\rho_{\tau^P}} \left( \frac{T10IShare_t}{T10IShare} \right)^{(1-\rho_{\tau^P})\gamma_W^{\tau^P}} \epsilon_t^P,$$

where the new parameter  $\gamma_W^{\tau^P}$  captures the response of tax progressivity to income inequality. Its prior follows a standard normal distribution. We find that tax progressivity does respond to the top 10 income share with an estimated elasticity of 0.41. In the US, the fiscal authority responds to higher income inequality by increasing the progressivity of taxes thereby mitigating the increase in pre-tax income inequality to post-tax income inequality. However, tax progressivity is still largely driven by exogenous shocks  $\epsilon_t^P$  as the feedback from inequality is quantitatively small.

### KPR PREFERENCES

The assumption of GHH preferences is mainly motivated by the fact that many estimated DSGE models of business cycles find small aggregate wealth effects in the labor supply; see, e.g., Schmitt-Grohé and Uribe (2012); Born and Pflieger (2014). Unfortunately, it is not feasible to estimate the flexible form of preference of Jaimovich and Rebelo (2009), which also encompasses King, Plosser and Rebelo (1988) (KPR) preferences. This would require solving the stationary equilibrium in every likelihood evaluation, which is substantially more time consuming than solving for the dynamics around this equilibrium. However, we estimate a version with KPR preferences; see below for details.

According to the marginal data density, the data clearly prefer the GHH specification over the KPR specification. What is more, the KPR version of the HANK model has more difficulty matching business cycle and inequality dynamics simultaneously.

The GHH assumption has been criticized by Auclert, Bardóczy and Rognlie (2023) on the basis of producing “too high” multipliers. In a companion paper (Bayer, Born and Luetticke, 2023), we show that our model produces multipliers of reasonable size both in the short and in the long run. The reason for this lies in the combination of model elements only briefly discussed or even absent in the stylized Auclert, Bardóczy and Rognlie (2023) economy: sticky wages, distortionary taxes, capacity utilization, and a Taylor rule. Capacity utilization allows for output adjustment without adjusting hours; additional wage stickiness translates increasing labor demand into higher wage markups instead of hours and consumption; distortionary taxes absorb an additional fraction of income; and the Taylor rule translates the fiscal shock into to a real interest rate increase. The back-of-the envelope calculation of the multiplier based on formula (15) in Auclert, Bardóczy and Rognlie (2023), counter-factually assuming fixed real rates and ignoring capacity utilization, would be:  $(1 - (1 - \tau)(\eta - 1)/\eta(\zeta - 1)/\zeta)^{-1} \approx 2.5$ . The true multiplier in the model with capacity utilization and interest rate response is, in line with the data, much smaller.

Changing the preferences to King, Plosser and Rebelo (1988) preferences (instead of Greenwood, Hercowitz and Huffman (1988)) also requires the recalibration of the steady state. The felicity function  $u$ , additively separable in consump-

tion and leisure, now reads:

$$(B.2) \quad u(c_{it}, n_{it}) = \frac{c_{it}^{1-\xi} - 1}{1-\xi} - \gamma^{shift} \frac{n_{it}^{1+\gamma} - 1}{1+\gamma},$$

with risk aversion parameter  $\xi > 0$  and inverse Frisch elasticity  $\gamma > 0$ . The first-order condition for labor supply is:

$$(B.3) \quad n_{it} = \left[ \frac{1}{\gamma^{shift}} u'(c)(1 - \bar{\tau}^P)(1 - \tau_t^L)(wh_{it})^{(1-\bar{\tau}^P)} \right]^{\left(\frac{1}{\gamma+\bar{\tau}^P}\right)}.$$

We recalibrate the steady state to match the capital-to-output ratio, the bonds-to-capital ratio, the fraction of borrowers, and the top 10 wealth share as reported in Table 1. This yields a discount factor of  $\beta = 0.988$ , a portfolio adjustment probability of  $\lambda = 8.25\%$ , a borrowing penalty of  $\bar{R} = 3.56\%$ , and a probability of becoming an entrepreneur of  $1/2000$ .

### B.2. Parameter estimates

Table B.5 displays the estimation results for the model variants. The estimated parameters are broadly similar across variants with some exceptions. The KPR estimates feature lower real frictions and a different parameterization of the tax rule.

TABLE B.5—POSTERIOR DISTRIBUTIONS: MODEL VARIANTS

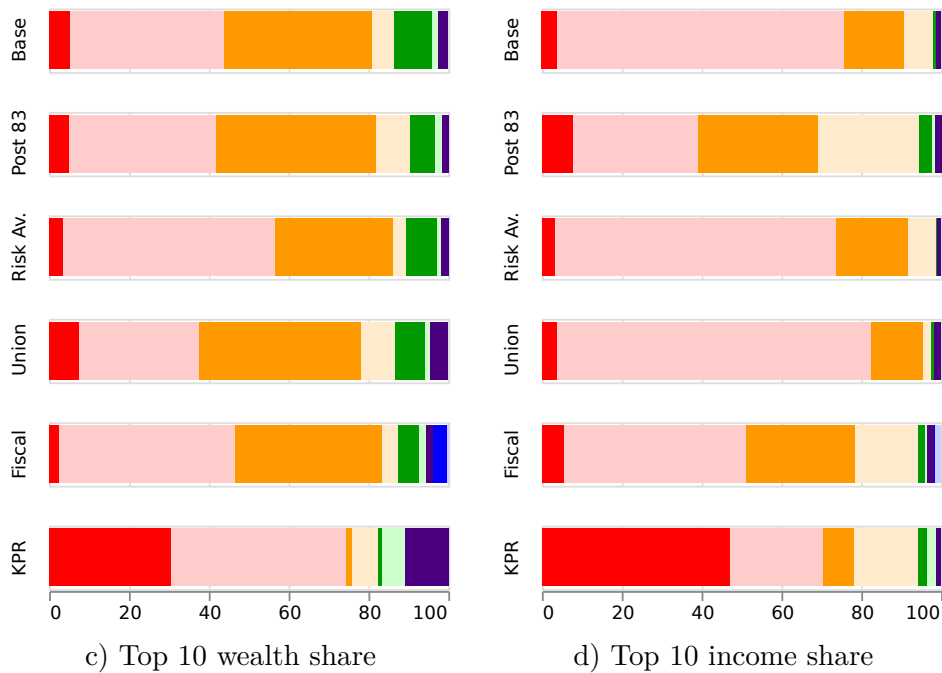
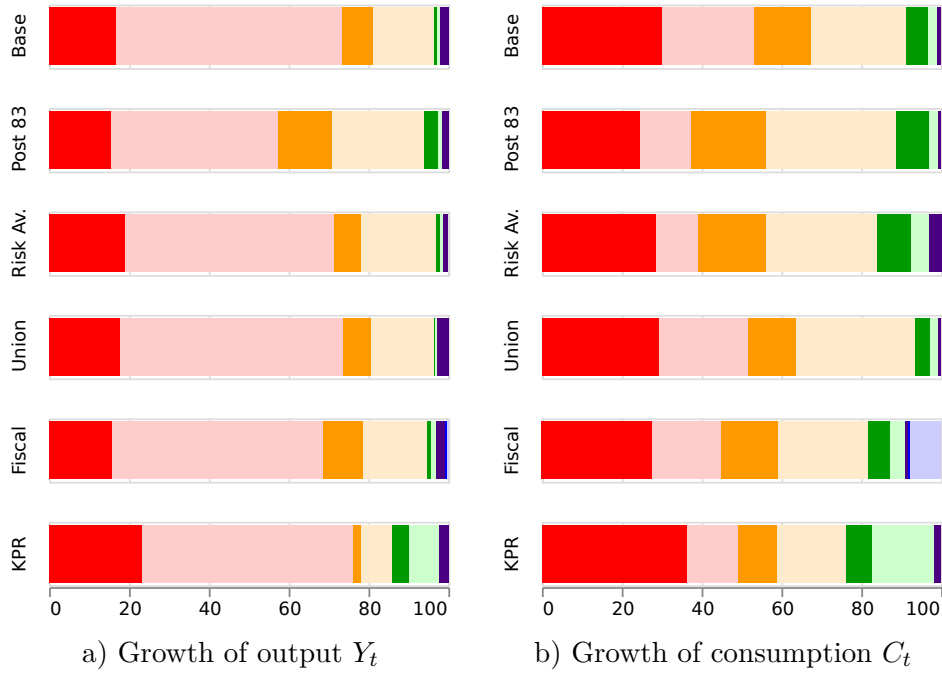
Parameter	Posterior				
	HANK (Post-83)	HANK (RA2)	HANK (Union)	HANK-X (Tax)	HANK (KPR)
Frictions					
$\delta_s$	1.060 (0.981, 1.137)	2.516 (1.937, 3.135)	0.929 (0.667, 1.237)	0.871 (0.588, 1.193)	0.168 (0.085, 0.268)
$\phi$	2.876 (2.168, 3.576)	3.429 (2.557, 4.332)	4.277 (3.427, 5.293)	2.493 (1.694, 3.334)	0.321 (0.212, 0.454)
$\kappa$	0.082 (0.057, 0.113)	0.217 (0.174, 0.264)	0.179 (0.138, 0.225)	0.151 (0.117, 0.188)	0.091 (0.078, 0.105)
$\kappa_w$	0.268 (0.197, 0.347)	0.318 (0.249, 0.392)	0.311 (0.243, 0.383)	0.253 (0.189, 0.321)	0.314 (0.241, 0.397)
$\iota\Pi$	0.693 (0.599, 0.786)	0.174 (0.021, 0.433)	0.298 (0.044, 0.673)	0.695 (0.342, 0.949)	0.205 (0.173, 0.234)
Debt and monetary policy rules					
$\rho_R$	0.862 (0.842, 0.881)	0.780 (0.751, 0.806)	0.781 (0.754, 0.806)	0.811 (0.785, 0.835)	0.736 (0.704, 0.766)
$\sigma_R$	0.136 (0.122, 0.153)	0.247 (0.226, 0.269)	0.230 (0.211, 0.251)	0.226 (0.208, 0.245)	0.264 (0.240, 0.289)
$\theta_\pi$	2.933 (2.636, 3.237)	2.164 (1.959, 2.389)	1.786 (1.578, 1.995)	2.024 (1.784, 2.273)	2.088 (1.931, 2.259)
$\theta_Y$	0.193 (0.119, 0.269)	0.197 (0.128, 0.265)	0.196 (0.130, 0.265)	0.212 (0.142, 0.282)	0.335 (0.275, 0.396)
$\gamma_B$	0.020 (0.004, 0.042)	0.088 (0.047, 0.133)	0.026 (0.003, 0.070)	0.007 (0.001, 0.023)	0.006 (0.001, 0.015)
$\gamma_\pi$	-2.334 (-2.671, -2.023)	-2.803 (-3.153, -2.474)	-3.085 (-3.583, -2.674)	-2.319 (-2.642, -2.037)	-1.90 (-2.06, -1.744)
$\gamma_Y$	-0.63 (-0.74, -0.528)	-0.822 (-0.922, -0.726)	-0.901 (-1.099, -0.735)	-0.533 (-0.69, -0.397)	-0.287 (-0.336, -0.241)
$\rho_D$	0.968 (0.938, 0.990)	0.969 (0.938, 0.991)	0.921 (0.878, 0.961)	0.950 (0.912, 0.985)	0.990 (0.980, 0.997)
$\sigma_D$	0.282 (0.218, 0.355)	0.481 (0.402, 0.568)	0.619 (0.524, 0.732)	0.422 (0.347, 0.508)	0.322 (0.286, 0.362)
Tax rules					
$\rho_\tau$	0.411 (0.276, 0.554)	0.270 (0.110, 0.429)	0.405 (0.212, 0.573)	0.422 (0.256, 0.570)	0.419 (0.409, 0.429)
$\gamma_B^T$	3.120 (3.068, 3.173)	2.270 (1.396, 3.233)	2.519 (1.511, 3.656)	3.098 (2.199, 4.059)	-0.202 (-0.219, -0.186)
$\gamma_Y^T$	0.788 (0.757, 0.818)	2.269 (2.160, 2.384)	1.976 (0.474, 3.357)	0.162 (-1.404, 1.662)	-0.455 (-0.471, -0.44)
$\rho_P$	— (—, —)	— (—, —)	— (—, —)	0.917 (0.882, 0.947)	— (—, —)
$\sigma_P$	— (—, —)	— (—, —)	— (—, —)	6.909 (5.870, 8.160)	— (—, —)
$\gamma_W^P$	— (—, —)	— (—, —)	— (—, —)	0.230 (-0.095, 0.532)	— (—, —)
Structural shocks					
$\rho_A$	0.942 (0.910, 0.969)	0.931 (0.897, 0.962)	0.961 (0.926, 0.990)	0.991 (0.973, 0.998)	0.942 (0.927, 0.956)
$\sigma_A$	0.178 (0.152, 0.209)	0.230 (0.187, 0.276)	0.175 (0.116, 0.244)	0.137 (0.109, 0.173)	0.164 (0.147, 0.182)
$\rho_Z$	0.995 (0.992, 0.998)	0.991 (0.988, 0.995)	0.997 (0.996, 0.999)	0.998 (0.997, 0.999)	0.880 (0.863, 0.896)
$\sigma_Z$	0.551 (0.491, 0.619)	0.611 (0.565, 0.661)	0.623 (0.572, 0.678)	0.597 (0.551, 0.646)	1.799 (1.651, 1.958)
$\rho_\Psi$	0.782 (0.710, 0.846)	0.703 (0.651, 0.754)	0.583 (0.513, 0.653)	0.729 (0.666, 0.793)	0.960 (0.953, 0.967)
$\sigma_\Psi$	6.869 (5.482, 8.415)	14.609 (11.338, 18.073)	14.961 (12.265, 18.149)	8.831 (6.444, 11.463)	3.629 (3.110, 4.225)
$\rho_\mu$	0.813 (0.759, 0.859)	0.897 (0.870, 0.922)	0.924 (0.903, 0.942)	0.901 (0.876, 0.923)	0.994 (0.962, 1.000)
$\sigma_\mu$	1.800 (1.457, 2.247)	1.143 (1.019, 1.287)	1.163 (1.028, 1.318)	1.323 (1.160, 1.516)	0.375 (0.314, 0.557)
$\rho_{\mu w}$	0.907 (0.875, 0.932)	0.921 (0.897, 0.943)	0.938 (0.912, 0.961)	0.895 (0.865, 0.920)	0.789 (0.745, 0.829)
$\sigma_{\mu w}$	3.944 (3.265, 4.803)	3.302 (2.900, 3.773)	3.133 (2.771, 3.566)	3.678 (3.136, 4.354)	3.032 (2.547, 3.606)
Income risk process					
$\rho_s$	— (—, —)	— (—, —)	— (—, —)	0.522 (0.451, 0.585)	— (—, —)
$\sigma_s$	— (—, —)	— (—, —)	— (—, —)	68.278 (60.81, 76.774)	— (—, —)
$\Sigma_y$	— (—, —)	— (—, —)	— (—, —)	22.216 (22.14, 22.293)	— (—, —)
Measurement errors					
$\sigma_{W10}^{me}$	— (—, —)	— (—, —)	— (—, —)	1.977 (1.620, 2.389)	— (—, —)
$\sigma_{I10}^{me}$	— (—, —)	— (—, —)	— (—, —)	8.122 (6.744, 9.741)	— (—, —)

Note: The standard deviations of the shocks and measurement errors have been transformed into percentages by multiplying by 100. HANK (Post-83): HANK model estimated on post-Volcker data only; HANK (RA2): HANK model with risk aversion 2 instead of 4; HANK (Union): HANK model in which union profits are payed out proportionally to idiosyncratic productivity; HANK-X (Tax): HANK-X model with income-inequality feedback to tax progressivity; HANK (KPR): HANK model with KPR instead of GHH preferences. For more details see text.

*B.3. Variance decompositions*

Figure B.15 shows that the variance decompositions are similar across all variants. Shocks to investment specific technology are by far the most important driver of output growth (explaining 40-60%), followed with some distance by shocks to TFP and wage markups. The same three shocks are prominent in consumption growth but of more equal importance and with TFP being the most important one. The variance decompositions of top 10 wealth and income shares are also quite similar. The outliers are KPR preferences and risk aversion 2. The former variant finds a larger role for TFP shocks in explaining inequality, while the latter finds a larger role for investment specific technology shocks.

FIGURE B.15. VARIANCE DECOMPOSITIONS: OUTPUT AND CONSUMPTION GROWTH



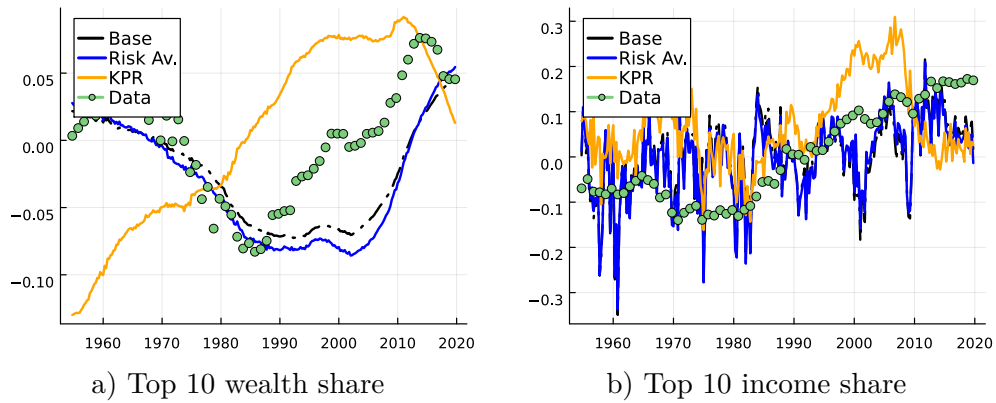
**Shock**

- tfp
- inv.-spec. tech.
- price markup
- wage markup
- risk premium
- mon. policy
- structural deficit
- tax prog.
- income risk

*Note:* Conditional variance decompositions at business cycle frequencies (6-32 quarter forecast horizon) for the baseline and the estimated variants 1) sample 1983-2019, 2) risk aversion 2, 3) proportional union profits, 4) fiscal policy reacts to inequality, 5) KPR preferences.

#### B.4. Historical decomposition of inequality

Figure B.16 shows the historical decomposition of inequality for these two variants, KPR and risk aversion 2, that differ most from the baseline in the previous section. Estimating the model with risk aversion 2 does not affect the implied time path of the top 10 income and wealth shares much. KPR preferences, however, do change the estimated results. Wealth inequality is now rising throughout the whole period, missing the U-shape. While income inequality is too high from 1970-2010 and too low afterwards such that the top 10 income share does not display a significant trend over the whole sample.



*Note:* Kalman smoother in comparison to the data for the top 10 wealth and income shares for the baseline and the estimated variants risk aversion 2 and KPR. Y-axis: Percent deviation from mean.

FIGURE B.16. HISTORICAL DECOMPOSITIONS: INEQUALITY

### C. Further details on the solution technique

#### C.1. Deviations of functionals from steady state

Our solution technique, following Reiter (2009), is based on writing the sequential equilibrium as a non-linear difference equation in function space. For this purpose, we write the marginal value functions,  $\frac{\partial \mathbb{W}_t}{\partial b}$  and  $\frac{\partial \mathbb{W}_t}{\partial k}$ , as a sum of the stationary equilibrium function,  $\bar{\mathbb{W}}_{b/k}$ , and time- $t$  deviations thereof,  $\hat{\mathbb{W}}_{b/k,t}$ . Since we work with Young's 2010 formulation of off-grid policies as fair gambles between grid points, we represent all functions as linear interpolants based on a set of node values for the full tensor grid of  $b, k, h$ . However, we represent the nodal values by their (3-dimensional) DCT coefficients, that is by the coefficients,  $\theta^{p,q,r}$ , of Chebychev polynomials,  $T_{p/q/r}(\cdot)$ , where we assume that the grid nodes were transformed to the corresponding Chebychev nodes:

$$(C.1) \quad \hat{\mathbb{W}}_{b/k,t}(b_i, k_j, h_l) = \sum_{p,q,r} \theta_{\hat{\mathbb{W}}_{b/k,t}}^{p,q,r} T_p(i) T_q(j) T_r(l).$$

The advantage of this formulation is that we can read off from the stationary equilibrium solution, which sparse polynomial would have been a good approximation to the non-sparse solution by comparing the absolute values of  $\theta^{p,q,r}$ . One way to do this is to look at the function values in the stationary distribution and fit the polynomials. If we had restricted the stationary equilibrium solution to the sparse polynomial class that forces the small coefficients to zero, then the solution would not have changed much. While we do not enforce this restriction in calculating  $\bar{\mathbb{W}}_{b/k}$ , we use it to select a baseline set of polynomials, i.e., the coefficients  $\theta^{p,q,r}$  in (C.1), to be perturbed when we linearize the system.

We add further perturbed coefficients based on how the multidimensional DCTs of the marginal value functions change, when prices change. For this purpose we calculate the discounted sum of expected changes in the marginal value functions and perform a multidimensional DCT on this object. In the next subsection, we discuss how this term is related to our ideal model reduction. This allows us to maintain a sparser basis than by just basing the selection on the steady state shape of the marginal value functions alone.

For the distribution function, we extend the approach of Bayer and Lueticke (2020). Again following Young (2010), we write the distribution function in terms of its histogram over the discrete nodes  $b, k, h$ . We then re-interpret this histogram as the histogram of its copula (i.e., the joint-distribution of marginal probabilities) by translating the axes from the  $b, k, h$  space to the space of the marginal distributions  $F_t^b, F_t^k, F_t^h$ . This allows us to split the joint distribution of  $b, k, h$  into three separate objects: First, marginal distributions at time  $t$ , second the copula in the stationary equilibrium  $\bar{C}(F_{i,t}^b, F_{j,t}^k, F_{l,t}^h)$ , at the grid points of  $b, k, h$  with indices  $i, j, l$  evaluated at these marginals and, third, deviations of the copula,  $\hat{C}_t$ .

The advantage of this splitting the distribution into three objects is that we can

work with different degrees of precision for the different objects. Again, we write all functionals as linear interpolants over a set of nodal values. The nodal values of  $\bar{C}$  are simply given by the stationary distribution. This means, we define the node grid  $\{F_i^b, F_j^k, F_l^h\}$  in line with the stationary marginal distributions over the  $b, k$ , and  $h$  grid, respectively.

The deviation of the copula is again given by a linear interpolant of the pdf  $d\hat{C}$  over nodal values represented by a discrete-cosine transform that uses a subset of the nodal grid of  $\bar{C}$ :

$$(C.2) \quad d\hat{C}_t(F_i^b, F_j^k, F_l^h) = \sum_{p,q,r} \theta_{C,t}^{p,q,r} T_p(i) T_q(j) T_r(l).$$

A sparser grid for  $\hat{C}$  implies that we need to perturb less coefficients. Working with the multidimensional DCT-transformation on top, allows us to easily formulate the constraints that are posed by making sure that the combined copula  $\bar{C} + \hat{C}$  remains a copula (fulfills the restrictions on partial integrals).<sup>2</sup> This constraint translates into parameter restrictions on  $\theta_{C,t}^{p,q,r}$ , where  $\theta_{C,t}^{p,q,r} = 0$  for  $p = q = 1$ ,  $q = r = 1$ , or  $p = r = 1$ . This restriction ensures that  $\int dC_t = 0$  and reflects that  $\sum_s T_s(m) = 0$  for  $s > 1$  where  $m$  is the Chebychev node index. The excluded coefficients are the only tensor basis elements that have non-zero marginals. We do not restrict the perturbed coefficients any further than this before running the second-step model reduction.

### C.2. Intuition for the possibility of a strong model reduction

The procedure above gives us the first-stage model reduction. It is based only on objects calculated from the stationary equilibrium. While this renders solving for a sequential equilibrium feasible, because the model becomes sufficiently small in terms of the number of variables involved, this number is still large and would thus yield long estimation times. Our second-stage model reduction leverages the Bayesian setup, using prior knowledge about the dynamics to derive a factor representation of the idiosyncratic model part. We find that it reduces the model dramatically in the number of variables, making estimation feasible.

To gain some intuition for why such strong further model reduction is possible, it is useful to draw insights from the sequence-space solution techniques (Auclert et al., 2021). The key idea, which sequence-space techniques leverage, is that the household’s decision problem depends only on the expected sequence of a small set of “prices”  $P_t$ .<sup>3</sup> We can use the envelop theorem, to calculate recursively the response of the value functions (or derivatives thereof) to a change in an expected future price  $P_{t+h}$ . Assuming that we wrote the problem such that prices do only

<sup>2</sup>Note, that different to Bayer and Luetticke (2020) we do not use the DCT on the copula for a first-stage model reduction but instead work with a coarser set of nodes and linear interpolations.

<sup>3</sup>These are: level and progressivity of taxes, income risk, wage rate, real interest rate on liquid assets, price of capital, return on capital, entrepreneurial profits, and union profits; see equation (36) for example.

show up contemporaneously in the Bellman equation, we have for  $h > 0$ :

$$(C.3) \quad \frac{\partial \mathbb{W}_t}{\partial P_{t+h}} = \left( \frac{\partial u}{\partial x_{t+1}} + \beta \Gamma \frac{\partial \mathbb{W}_{t+1}}{\partial x_{t+1}} \right) \frac{\partial x_{t+1}}{\partial P_{t+h}} + \beta \Gamma \frac{\partial \mathbb{W}_{t+1}}{\partial P_{t+h}},$$

where  $\Gamma$  is the transition matrix induced by stationary equilibrium policies and income shocks (i.e., it includes the expectations operator). Here,  $x_{t+1}$  are the endogenous idiosyncratic states. Importantly, the sum of the first two terms is zero when the choice of  $x_{t+1}$  is not constrained because the borrowing constraint does not bind. When it binds, however,  $\frac{\partial x_{t+1}}{\partial P_{t+h}} = 0$ . This implies that the product of the two terms is always zero and we can write  $\frac{\partial \mathbb{W}_t}{\partial P_{t+h}}$  recursively as

$$(C.4) \quad \frac{\partial \mathbb{W}_t}{\partial P_{t+h}} = \beta^h \Gamma^h \underbrace{\frac{\partial \mathbb{W}_t}{\partial P_t}}_{=: \mathbf{w}_P}.$$

The sequence-space method assumes that it is possible to approximate the impact of a shock by a finite  $T$  period sequence of prices. Given this assumption, we know that we can write the equilibrium sequence of prices as an impulse response

$$(C.5) \quad \mathbb{E}_t dP_{t+h} = \Phi_h \epsilon_t.$$

Stability requires that  $\lim_{h \rightarrow \infty} \Phi_h = 0$  and if the sequence-space solution is exact at horizon  $T$ ,  $\Phi_h \approx 0 \quad \forall h \geq T$ .

If we now consider infinitesimally small shocks, we can write the deviations of the value functions (in a total differential notation) as

$$(C.6) \quad \begin{aligned} d\mathbb{W}_t &= \mathbb{E}_t \sum_{h=0}^T \frac{\partial \mathbb{W}_t}{\partial P_{t+h}} dP_{t+h} = \mathbb{E}_t \sum_{h=0}^T (\beta \Gamma)^h \mathbf{w}_P dP_{t+h} \\ &= \sum_{h=0}^T (\beta \Gamma)^h \mathbf{w}_P \sum_{s=0}^T \Phi_{s+h} \epsilon_{t-s} = \underbrace{\sum_{s=0}^T \sum_{h=0}^{T-s} (\beta \Gamma)^h \mathbf{w}_P \Phi_{s+h} \epsilon_{t-s}}_{=: C_s}. \end{aligned}$$

The second equality uses the envelope result from (C.4). The third equality first replaces the change in future prices by the impulse responses to contemporaneous and past shocks according to (C.5). The last equality rearranges the sums using the truncation of the impulse responses at the horizon  $T$ .

This implies a structure for the variance covariance matrix of deviations in the

value functions:

$$(C.7) \quad \mathbb{E}d\mathbb{W}_t d\mathbb{W}'_t = [C_0 \quad \cdots \quad C_T] \begin{bmatrix} \Sigma_\epsilon & \cdots & 0 \\ 0 & \ddots & 0 \\ 0 & \cdots & \Sigma_\epsilon \end{bmatrix} \begin{bmatrix} C'_0 \\ \vdots \\ C'_T \end{bmatrix} = \sum_{s=0}^T C_s \Sigma_\epsilon C'_s.$$

Since the rank of a sum of matrices is bounded from above by the sum of the ranks, and each summand in (C.7) has rank  $J$ , the variance covariance matrix of the value functions has at most rank  $T \times J$ , where  $J$  is the number of shocks. This means that, under the assumption that a  $T$ -period approximation is good enough (for a sequence-space solution), there are at most  $T \times J$  factors in the value functions.

This upper bound is, however, loose: The increments in the matrix sums  $C_s$  shrink in  $s$  towards zero because of discounting in the planning problem,  $\lim_{s \rightarrow \infty} \beta^s = 0$ , and the stability of the price process,  $\lim_{h \rightarrow \infty} \Phi_h = 0$ . This effectively means that  $C_s$  converges more quickly to a constant than  $\Phi_s$  or  $\beta^s$  alone and the sum (C.7) can be approximated well using a smaller  $T$  than the actual truncation horizon.

The special case where we can write the impulse-response of the prices in terms of a VAR(1) in  $F$  prices (potentially in companion form) is particularly illustrative for the strength of the model reduction. In that case, we obtain the impulse responses as  $\Phi_h = \Phi^h$  and (C.6) and (C.7) can be further simplified to

$$(C.8) \quad d\mathbb{W}_t = \sum_{h=0}^T (\beta\Gamma)^h \mathbf{w}_P \sum_{s=0}^T \Phi_{s+h} \epsilon_{t-s} = \underbrace{\sum_{h=0}^T (\beta\Gamma)^h \mathbf{w}_P \Phi^h}_{=: \bar{C}} \sum_{s=0}^T \Phi^s \epsilon_{t-s}$$

$$\mathbb{E}d\mathbb{W}_t d\mathbb{W}'_t = \bar{C} \left[ \sum_{s=0}^T \Phi^s \Sigma_\epsilon \Phi'^s \right] \bar{C}'.$$

Since the inner term in brackets is of size  $F \times F$ , the variance-covariance matrix of the value functions has at most rank  $F$ . This explains why in practice the reduction retains only few more factors than the number of prices and thus is far below  $T \times J$ .

Of course, in actually solving the model, we work with the marginal values instead of the value functions, but the arguments for the number of factors in the value functions carry over to their marginals. Applying the chain rule, we observe

for  $h > 0$ :

$$\begin{aligned}
 \text{(C.9)} \\
 \frac{\partial}{\partial x} \frac{\partial \mathbb{W}_t}{\partial P_{t+h}}(b, k, h) &= \frac{\partial}{\partial x} \beta \mathbb{E} \frac{\partial \mathbb{W}_{t+1}}{\partial P_{t+h}}(b', k', h') \\
 &= \beta \lambda \left[ \frac{\partial b_a^*}{\partial x} \mathbb{E} \frac{\partial}{\partial b} \frac{\partial \mathbb{W}_{t+1}}{\partial P_{t+h}}(b_a^*, k^*, h') + \frac{\partial k^*}{\partial x} \mathbb{E} \frac{\partial}{\partial k} \frac{\partial \mathbb{W}_{t+1}}{\partial P_{t+h}}(b_a^*, k^*, h') \right] , \\
 &+ \beta(1 - \lambda) \left[ \frac{\partial b_n^*}{\partial x} \mathbb{E} \frac{\partial}{\partial b} \frac{\partial \mathbb{W}_{t+1}}{\partial P_{t+h}}(b_n^*, k, h') + \frac{\partial k}{\partial x} \mathbb{E} \frac{\partial}{\partial k} \frac{\partial \mathbb{W}_{t+1}}{\partial P_{t+h}}(b_n^*, k, h') \right]
 \end{aligned}$$

where  $x$  is either  $b$  or  $k$  and  $\frac{\partial b'}{\partial x}$  and  $\frac{\partial k'}{\partial x}$  show how the policy functions change.

This, we can bring again in matrix notation in a recursive form

$$\begin{aligned}
 \text{(C.10)} \\
 \begin{bmatrix} \frac{\partial}{\partial b} \frac{\partial \mathbb{W}_t}{\partial P_{t+h}} \\ \frac{\partial}{\partial k} \frac{\partial \mathbb{W}_t}{\partial P_{t+h}} \end{bmatrix} &= \beta \underbrace{\left( \lambda \begin{bmatrix} D_{b_a, b} \Gamma_a & D_{k_a, b} \Gamma_a \\ D_{b_a, k} \Gamma_a & D_{k_a, k} \Gamma_a \end{bmatrix} + (1 - \lambda) \begin{bmatrix} D_{b_n, b} \Gamma_n & 0 \\ D_{b_n, k} \Gamma_n & \Gamma_n \end{bmatrix} \right)}_{=: \tilde{\Gamma}} \begin{bmatrix} \frac{\partial}{\partial b} \frac{\partial \mathbb{W}_{t+1}}{\partial P_{t+h}} \\ \frac{\partial}{\partial k} \frac{\partial \mathbb{W}_{t+1}}{\partial P_{t+h}} \end{bmatrix} , \\
 &= \beta \tilde{\Gamma} \begin{bmatrix} \frac{\partial}{\partial b} \frac{\partial \mathbb{W}_{t+1}}{\partial P_{t+h}} \\ \frac{\partial}{\partial k} \frac{\partial \mathbb{W}_{t+1}}{\partial P_{t+h}} \end{bmatrix} = \left( \beta \tilde{\Gamma} \right)^h \begin{bmatrix} \frac{\partial}{\partial b} \frac{\partial \mathbb{W}_t}{\partial P_t} \\ \frac{\partial}{\partial k} \frac{\partial \mathbb{W}_t}{\partial P_t} \end{bmatrix}
 \end{aligned}$$

where  $D_{x,y}$  are diagonal matrices that contain the derivatives of the policy function  $x$  to argument  $y$  at each point  $(b, k, h)$ . The matrices  $\Gamma_a$  and  $\Gamma_n$  are the transition matrices conditional on adjustment and non-adjustment, respectively. The structure of (C.10) is the same as (C.4). This we can use to obtain an approximation to the analogue to  $\bar{C}$  to select additional DCT-coefficients for the first stage reduction as discussed in the preceding subsection. Here, we calculate  $\hat{C} = (I - \phi \beta \tilde{\Gamma})^{-1} \begin{bmatrix} \frac{\partial}{\partial b} \frac{\partial \mathbb{W}_t}{\partial P_t} \\ \frac{\partial}{\partial k} \frac{\partial \mathbb{W}_t}{\partial P_t} \end{bmatrix}$  where we assume an auxiliary ad-hoc AR(1) structure for prices with an AR(1) coefficient  $\phi = 0.999$ .

The general argument for reduction can be made for the variance covariance matrix of the distribution, too. Here, the upper bound is  $2 \times T \times J$ . As with the value function, in each period shocks of up to  $T$  periods in the past affect the households' decision and thus the distribution directly. Additionally, because the distribution itself is a state with memory that can be truncated at  $T$  periods, it accumulates these direct effects of past shocks for  $T$  periods. As a result, only shocks further in the past than  $t - 2T$  have no impact on the distribution.

This can be expressed formally as follows:

$$\begin{aligned}
d\Theta_t &= \sum_{h=0}^T \Gamma^{h'} d\Gamma'_{t-h} \bar{\Theta} = \sum_{h=0}^T \Gamma^{h'} \left[ \frac{\partial \Gamma' \bar{\Theta}}{\partial P} dP_{t-h} + \frac{\partial \Gamma' \bar{\Theta}}{\partial \mathbb{W}_{+1}} \mathbb{E}_{t-h} d\mathbb{W}_{t-h+1} \right] \\
&= \sum_{h=0}^T \Gamma^{h'} \left[ \frac{\partial \Gamma' \bar{\Theta}}{\partial P} \sum_{j=0}^T \Phi_j \epsilon_{t-h-j} + \frac{\partial \Gamma' \bar{\Theta}}{\partial \mathbb{W}_{+1}} \sum_{j=0}^T C_{j+1} \epsilon_{t-h-j} \right] \\
\text{(C.11)} \quad &= \sum_{h=0}^T \sum_{j=0}^T \Gamma^{h'} \left[ \frac{\partial \Gamma' \bar{\Theta}}{\partial P} \Phi_j + \frac{\partial \Gamma' \bar{\Theta}}{\partial \mathbb{W}_{+1}} C_{j+1} \right] \epsilon_{t-h-j} \\
&= \sum_{s=0}^{2T} \underbrace{\sum_{h=0}^s \sum_{j=0}^{s-h} \left[ \frac{\partial \Gamma' \bar{\Theta}}{\partial P} \Phi_j + \frac{\partial \Gamma' \bar{\Theta}}{\partial \mathbb{W}_{+1}} C_{j+1} \right]}_{=: D_s} \epsilon_{t-s} = \sum_{s=0}^{2T} D_s \epsilon_{t-s},
\end{aligned}$$

where the first equation expresses changes in the distribution  $d\Theta_t$  as changes in the transition matrix,  $d\Gamma'_{t-h}$ ,  $h$  periods before  $t$  that translate into period  $t$  changes through the repeated steady state transition matrix  $\Gamma^h$ . There are no cross terms, where marginal changes in the transition matrix interact with past marginal changes in the distribution because we look at a linearized solution. The second equation replaces the changes in the transition matrix in  $t-h$  by the partial direct effect of prices in that period  $\frac{\partial \Gamma' \bar{\Theta}}{\partial P} dP_{t-h}$  plus an indirect effect, where  $\partial \mathbb{W}_{+1}$  denotes the partial derivative with respect to the continuation value. The next equation makes use of the impulse response representation of prices and (C.6) to express changes in the continuation value as a function of past shocks. The next equations simply reorder the sums. The variance-covariance matrix of  $d\Theta_t$  therefore has, along the lines of the argument made for (C.7) a rank below  $2 \times T \times J$ .

As before, the bound is loose, because of three reasons: first the stability of the price process, second the convergence of  $\Gamma^h$  to a matrix with identical rows,  $\bar{\Theta}$ , and third the fact that when summing over grid points  $\sum \frac{\partial \Gamma' \bar{\Theta}}{\partial P} = \sum \frac{\partial \Gamma' \bar{\Theta}}{\partial \mathbb{W}_{+1}} = 0$  because the total mass of the distribution cannot change. However, as the discount factor does not appear directly, we can expect slower convergence of  $D_s$  than  $C_s$ .

### C.3. Intuition for local invariance of model reduction

What is important, in both (C.7) and (C.11) the parameters we estimate only enter through their effect on price dynamics  $\Phi_h$ . They affect neither the stationary equilibrium transition matrix  $\Gamma$ , nor the response of the value functions to price changes  $\mathbf{w}_P$ , and they also have no effect on how the optimal household policy responds to price or continuation value changes,  $\frac{\partial \Gamma' \bar{\Theta}}{\partial P_i}$  and  $\frac{\partial \Gamma' \bar{\Theta}}{\partial \mathbb{W}_{+1}}$ .

While the price dynamics change in parameters, their changes are bounded.

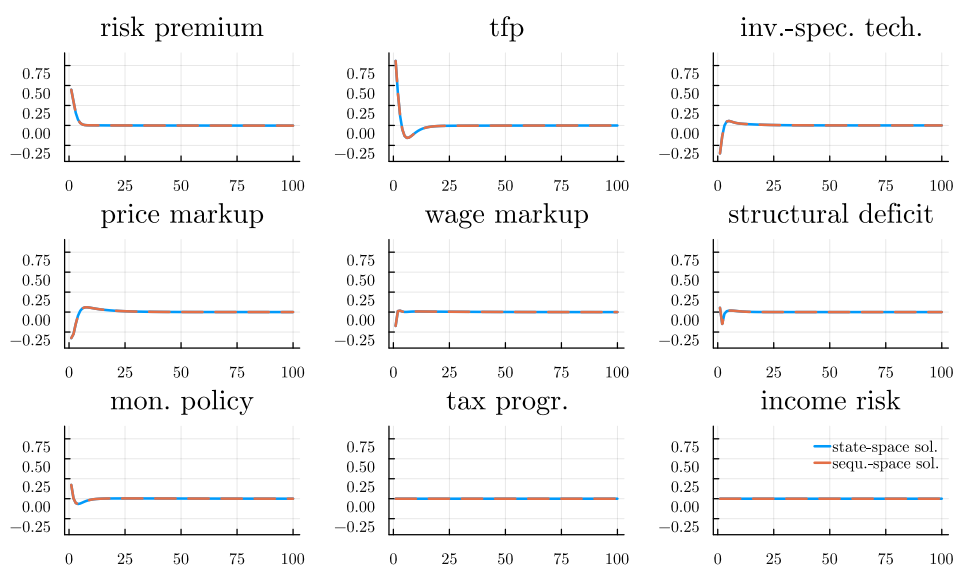
The priors, the model structure, and the data impose a restriction on how much the price process (C.5) changes between two likelihood evaluations. This implies that an ideal reduction basis, that is ultimately linked to the  $C_s$  and  $D_s$  of the preceding subsection, obtained under one set of parameters can be expected to remain a good basis in their vicinity. This is indeed what we observe in our application and the quality of the reduction basis can be verified ex post along the lines described in the main text.

#### C.4. *Direct IRF comparison across solution techniques*

Figures C.17 to C.20 compare the impulse responses of the observables used in the estimation of the HANK model obtained from our solution method to those obtained from a sequence-space method assuming a 300 period transition. The terminal values are assumed to be given by the state-space solution instead of the stationary equilibrium. The figures are organized by observable variables and show the responses to the various shocks in one figure. Figures C.21 to C.26 repeat this exercise for the HANK-X estimates.

The figures show that the differences in the IRFs are almost zero. What the IRFs also show is that the TFP shock leads to a persistent change in the capital stock (which can be seen in the persistent increase of employment). We also compared the sequence space solution with a 300 period transition to itself using the state-space solution as terminal outcome and the stationary equilibrium. Given the persistent change in the capital stock after a TFP shock, a 300 periods transition is not a good approximation and we find that the approximation error between the two solutions is for persistent variables more than one order of magnitude larger than between sequence and state-space solution. Results are available upon request.

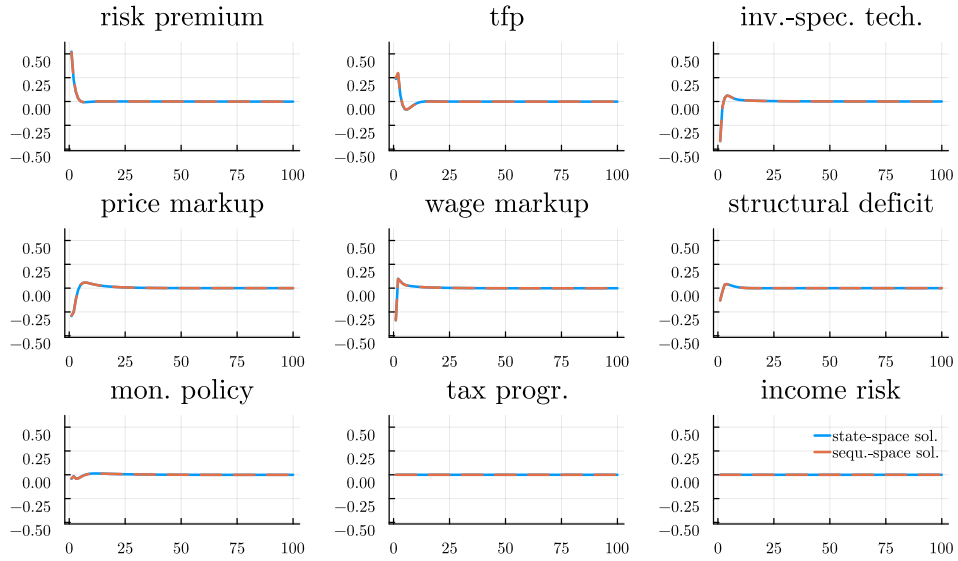
## Output growth response to a shock to ...



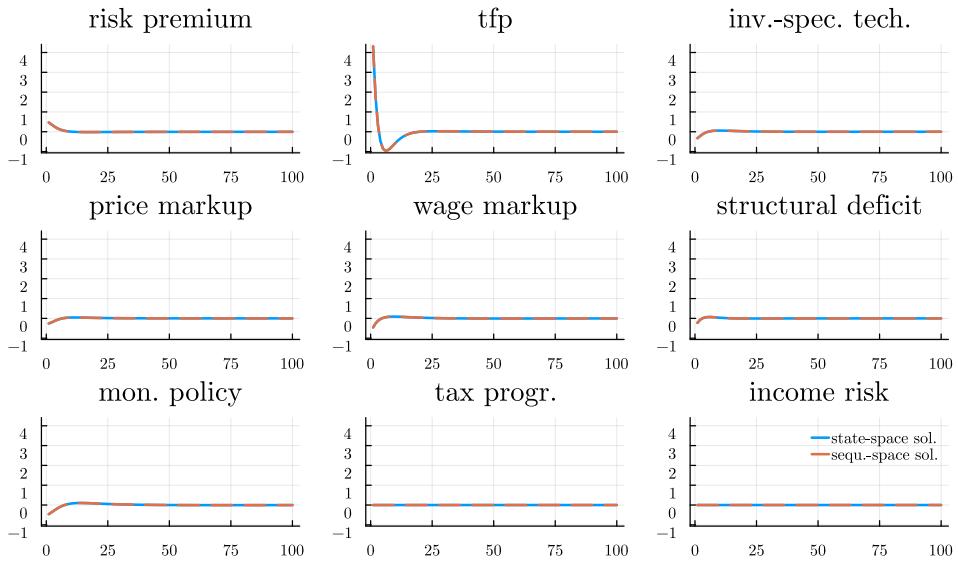
*Note:* The figure shows the impulse response to the various shocks in the HANK model, comparing a sequence-space solution (red dashed line) to our state-space solution (blue solid).

FIGURE C.17. COMPARISON OF IRFS ACROSS SOLUTION METHODS (HANK MODEL)

Consumption growth response to a shock to ...



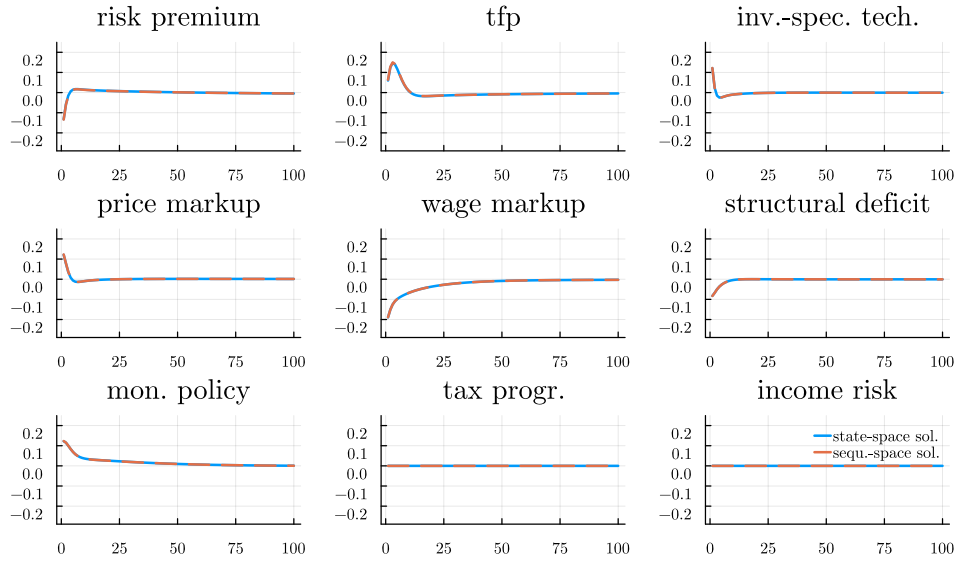
Investment growth response to a shock to ...



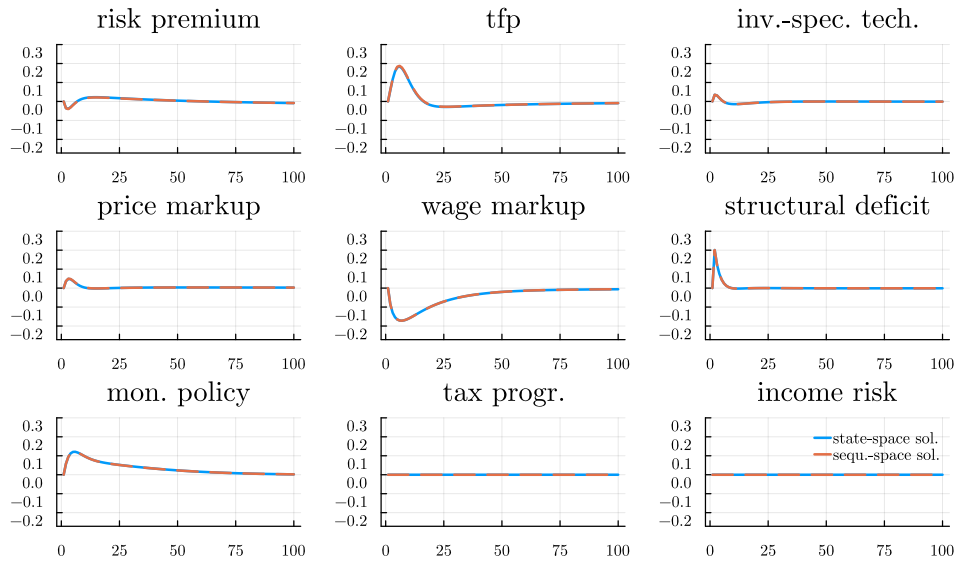
*Note:* The figure shows the impulse response to the various shocks in the HANK model, comparing a sequence-space solution (red dashed line) to our state-space solution (blue solid).

FIGURE C.18. COMPARISON OF IRFS ACROSS SOLUTION METHODS (HANK MODEL)

## Inflation response to a shock to ...



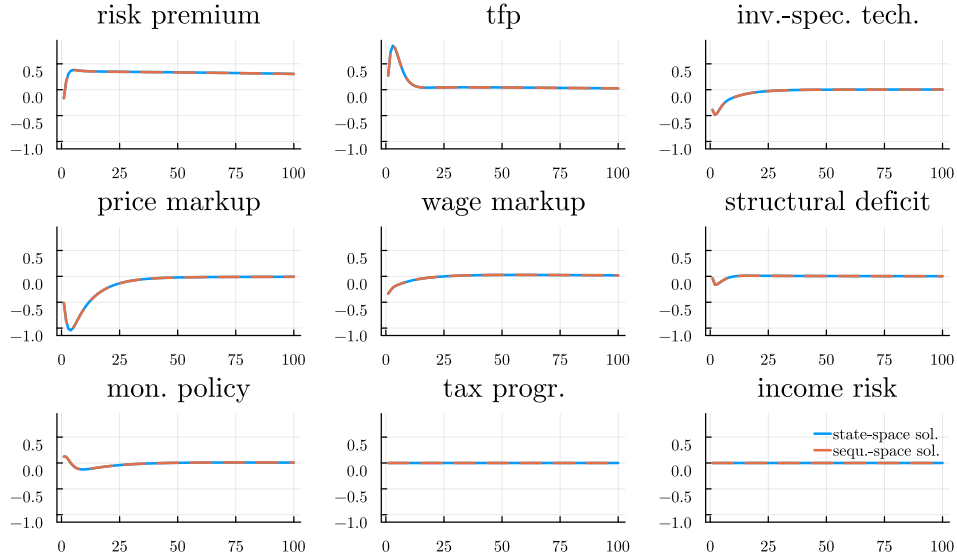
## Nominal rate response to a shock to ...



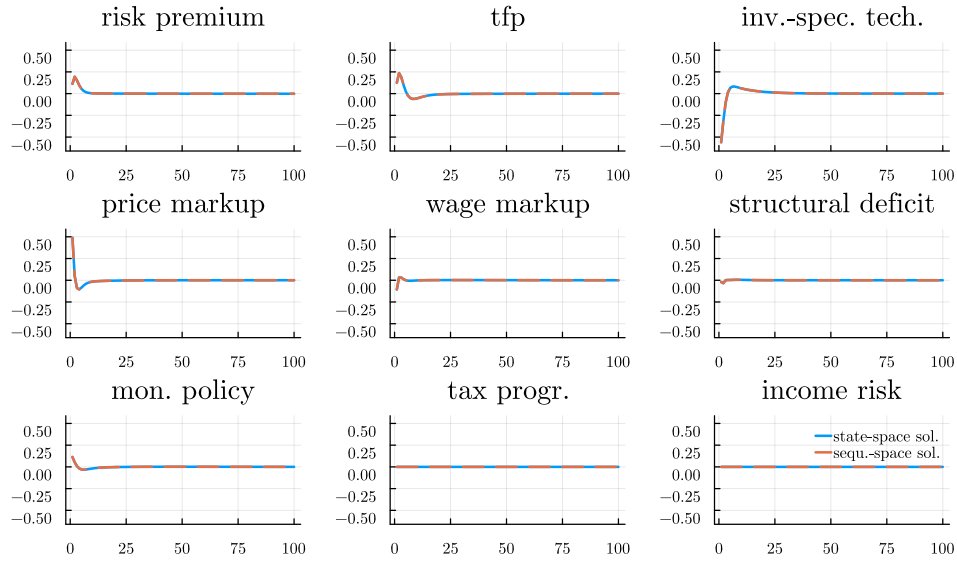
*Note:* The figure shows the impulse response to the various shocks in the HANK model, comparing a sequence-space solution (red dashed line) to our state-space solution (blue solid).

FIGURE C.19. COMPARISON OF IRFs ACROSS SOLUTION METHODS (HANK MODEL)

Employment response to a shock to ...



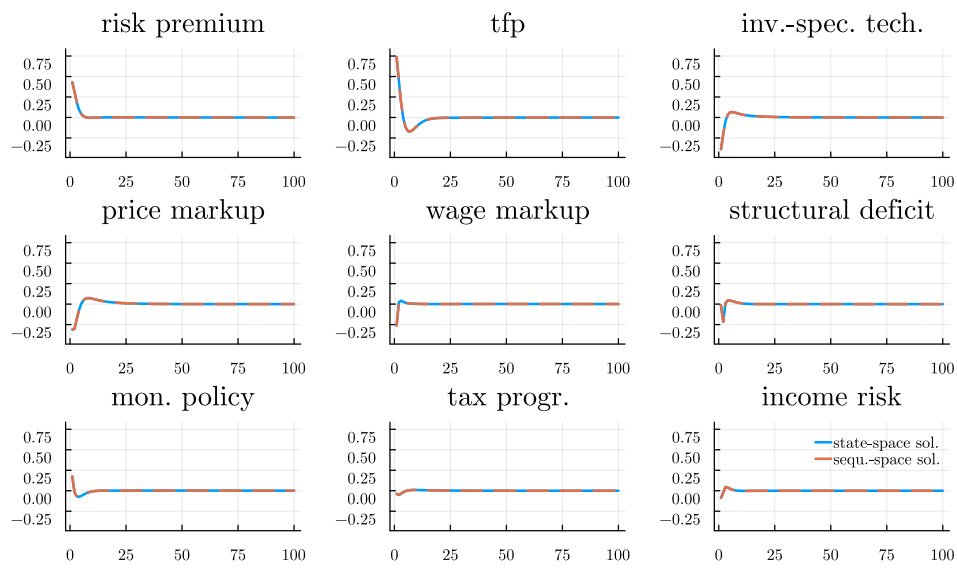
Wage growth response to a shock to ...



Note: The figure shows the impulse response to the various shocks in the HANK model, comparing a sequence-space solution (red dashed line) to our state-space solution (blue solid).

FIGURE C.20. COMPARISON OF IRFs ACROSS SOLUTION METHODS (HANK MODEL)

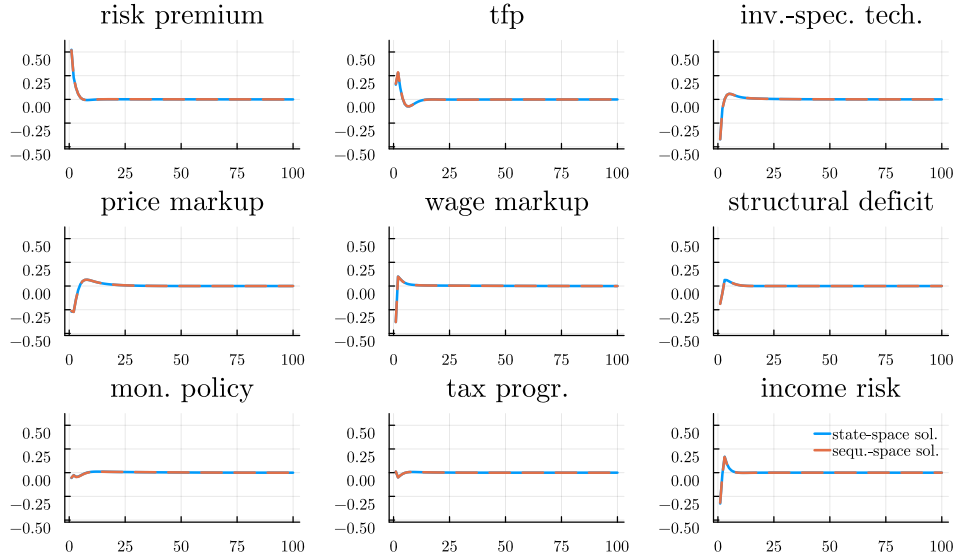
## Output growth response to a shock to ...



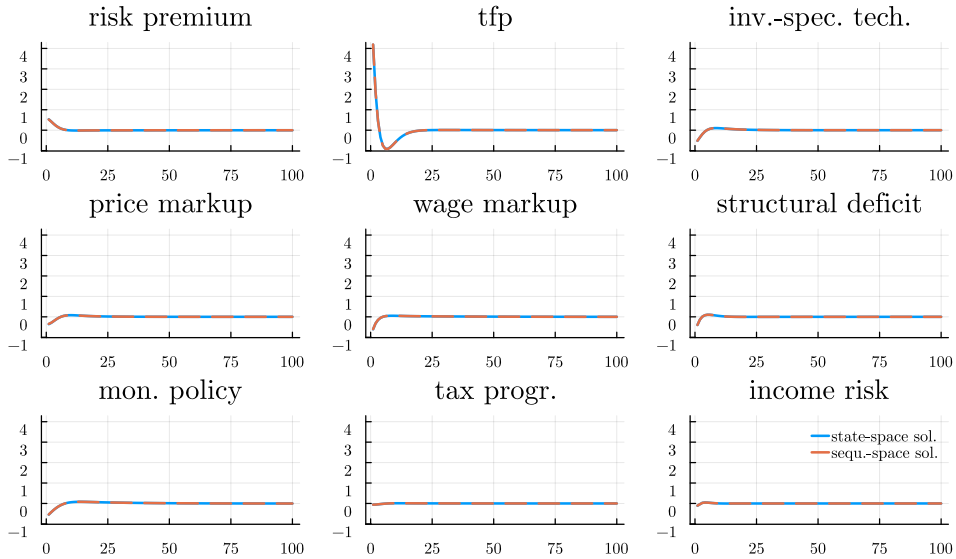
*Note:* The figure shows the impulse response to the various shocks in the HANK-X model, comparing a sequence-space solution (red dashed line) to our state-space solution (blue solid).

FIGURE C.21. COMPARISON OF IRFS ACROSS SOLUTION METHODS (HANK-X MODEL)

Consumption growth response to a shock to ...



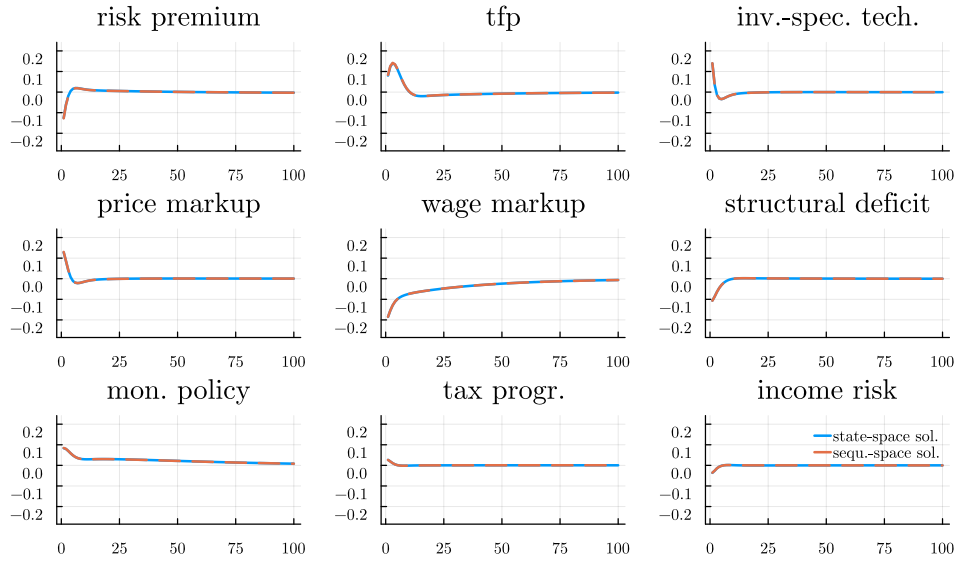
Investment growth response to a shock to ...



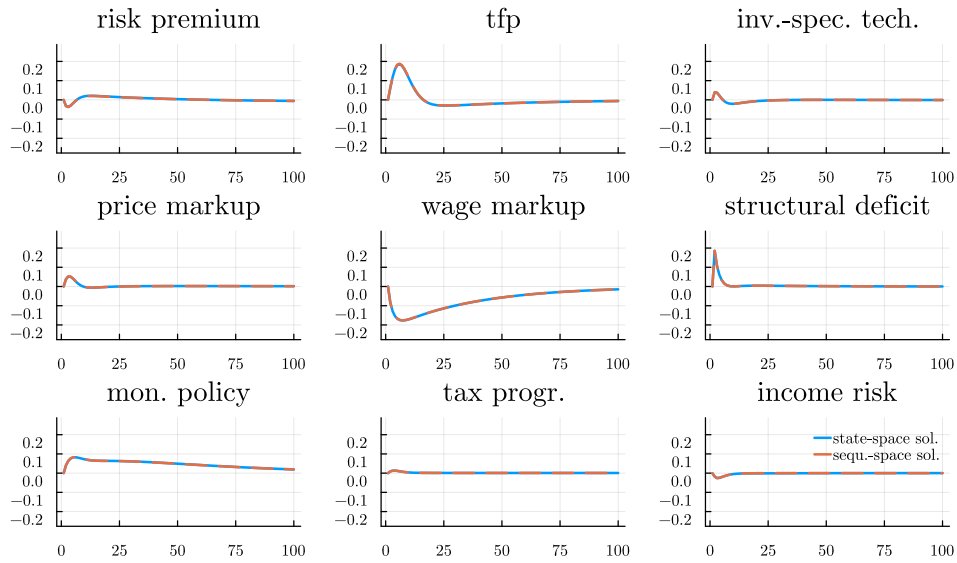
Note: The figure shows the impulse response to the various shocks in the HANK-X model, comparing a sequence-space solution (red dashed line) to our state-space solution (blue solid).

FIGURE C.22. COMPARISON OF IRFS ACROSS SOLUTION METHODS (HANK-X MODEL)

## Inflation response to a shock to ...



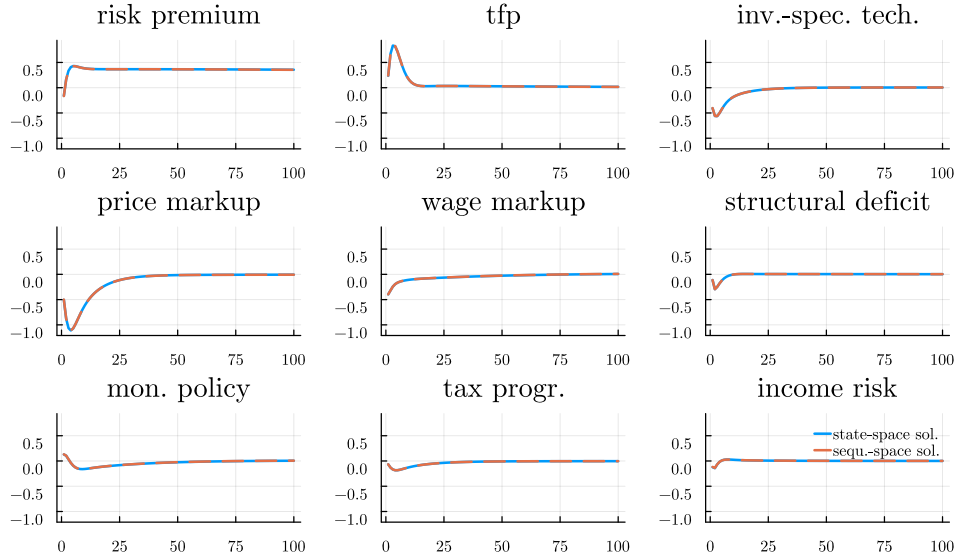
## Nominal rate response to a shock to ...



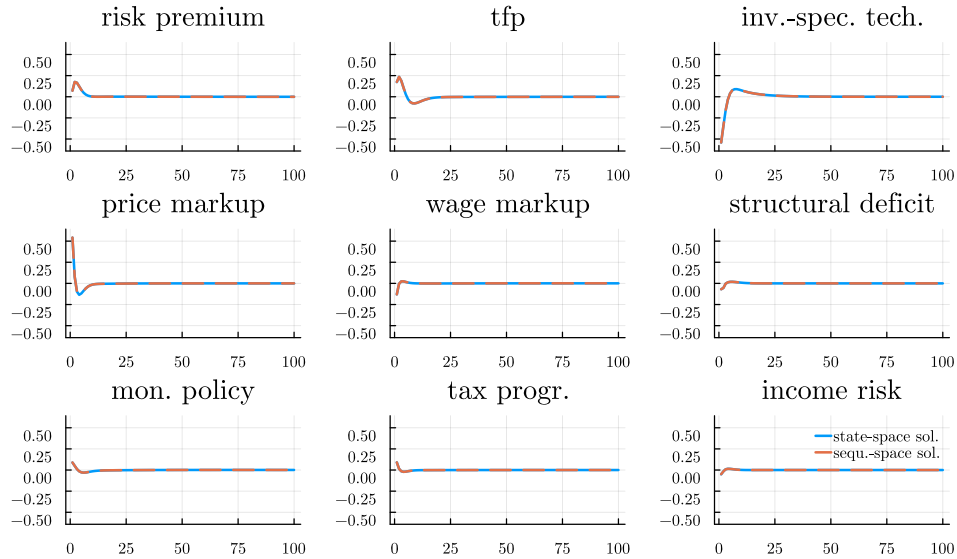
*Note:* The figure shows the impulse response to the various shocks in the HANK-X model, comparing a sequence-space solution (red dashed line) to our state-space solution (blue solid).

FIGURE C.23. COMPARISON OF IRFS ACROSS SOLUTION METHODS (HANK-X MODEL)

Employment response to a shock to ...



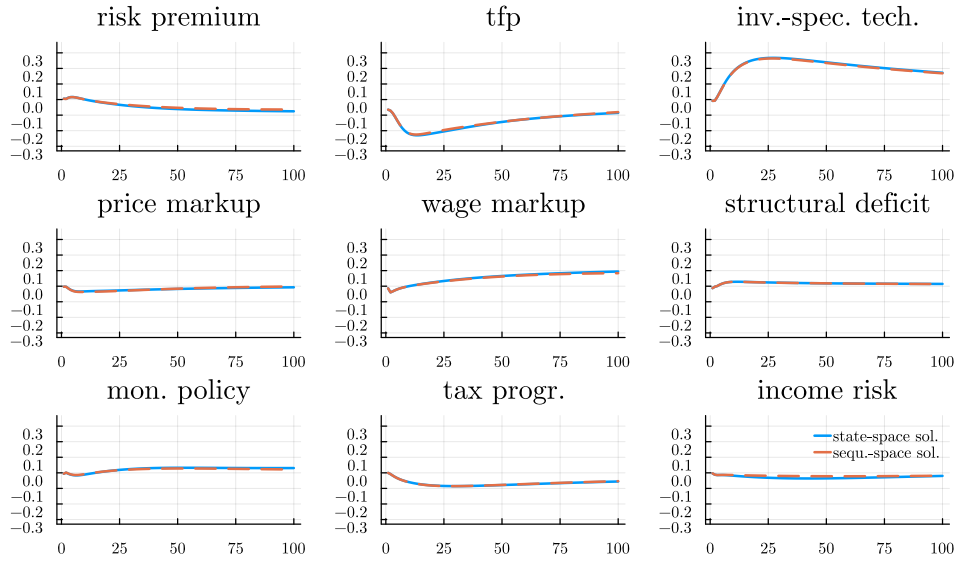
Wage growth response to a shock to ...



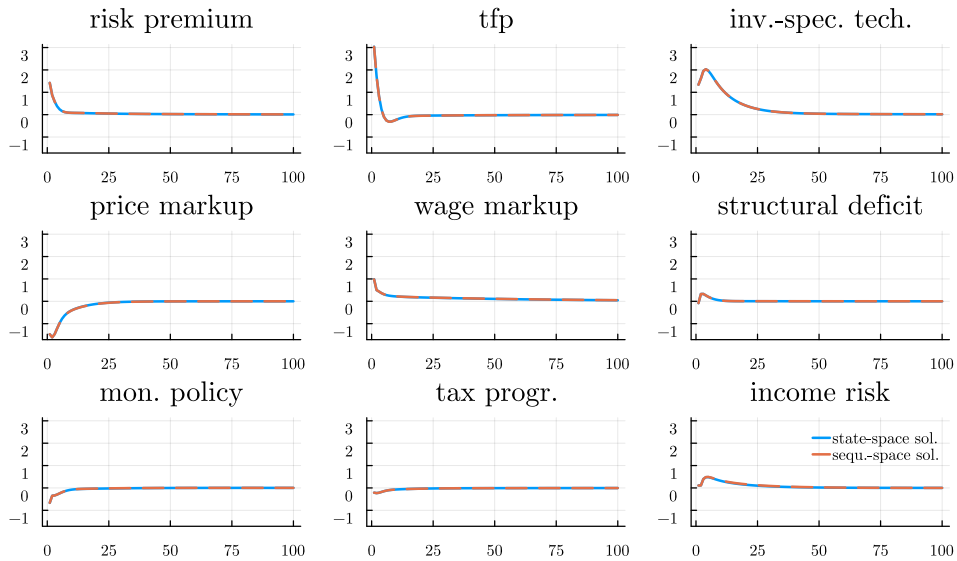
Note: The figure shows the impulse response to the various shocks in the HANK-X model, comparing a sequence-space solution (red dashed line) to our state-space solution (blue solid).

FIGURE C.24. COMPARISON OF IRFS ACROSS SOLUTION METHODS (HANK-X MODEL)

## T10 wealth share response to a shock to ...



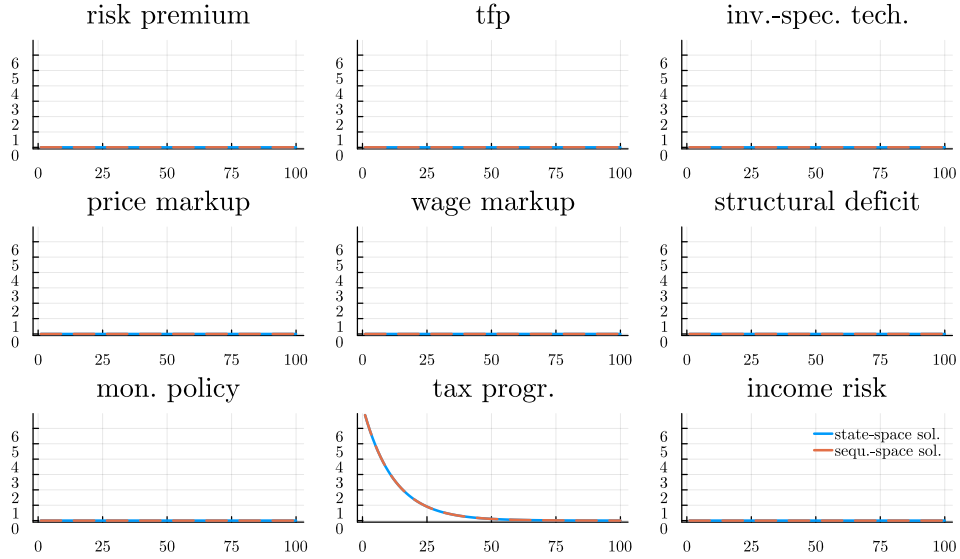
## T10 income share response to a shock to ...



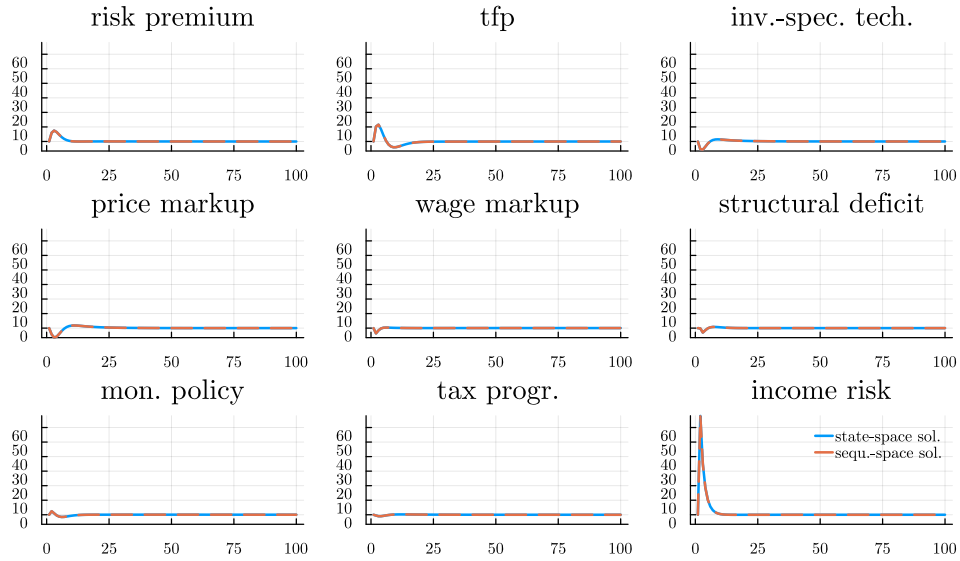
*Note:* The figure shows the impulse response to the various shocks in the HANK-X model, comparing a sequence-space solution (red dashed line) to our state-space solution (blue solid).

FIGURE C.25. COMPARISON OF IRFS ACROSS SOLUTION METHODS (HANK-X MODEL)

Tax progressivity response to a shock to ...



Income risk response to a shock to ...



Note: The figure shows the impulse response to the various shocks in the HANK-X model, comparing a sequence-space solution (red dashed line) to our state-space solution (blue solid).

FIGURE C.26. COMPARISON OF IRFS ACROSS SOLUTION METHODS (HANK-X MODEL)

## REFERENCES

- Auclert, Adrien, Bence Bardóczy, and Matthew Rognlie.** 2023. “MPCs, MPEs, and Multipliers: A Trilemma for New Keynesian Models.” *Review of Economics and Statistics*, 105(3): 700–71.
- Auclert, Adrien, Bence Bardóczy, Matthew Rognlie, and Ludwig Straub.** 2021. “Using the Sequence-Space Jacobian to Solve and Estimate Heterogeneous-Agent Models.” *Econometrica*, 89(5): 2375–2408.
- Bayer, Christian, and Ralph Luetticke.** 2020. “Solving Heterogeneous Agent Models in Discrete Time with Many Idiosyncratic States by Perturbation Methods.” *Quantitative Economics*, 11: 1253–1288.
- Bayer, Christian, Benjamin Born, and Ralph Luetticke.** 2023. “The Liquidity Channel of Fiscal Policy.” *Journal of Monetary Economics*, 134: 86–117.
- Bayer, Christian, Ralph Luetticke, Lien Pham-Dao, and Volker Tjaden.** 2019. “Precautionary Savings, Illiquid Assets, and the Aggregate Consequences of Shocks to Household Income Risk.” *Econometrica*, 87(1): 255–290.
- Board of Governors of the Federal Reserve System (U.S.).** 2023. “H.15 Selected Interest Rates.” Online Data Base. FEDFUNDS: <https://fred.stlouisfed.org/series/FEDFUNDS> (accessed Feb 16, 2023).
- Born, B., and J. Pfeifer.** 2014. “Policy Risk and the Business Cycle.” *Journal of Monetary Economics*, 68: 68–85.
- Chetty, Raj, Adam Guren, Day Manoli, and Andrea Weber.** 2011. “Are Micro and Macro Labor Supply Elasticities Consistent? A Review of Evidence on the Intensive and Extensive Margins.” *American Economic Review*, 101(3): 471–475.
- Ferriere, Axelle, and Gaston Navarro.** 2023. “The Heterogeneous Effects of Government Spending: It’s All About Taxes.” *Review of Economic Studies*, forthcoming.
- Geweke, John.** 1992. “Evaluating the Accuracy of Sampling-Based Approaches to the Calculation of Posterior Moments.” In *Bayesian Statistics*. Vol. 4, , ed. José M. Bernardo, James O. Berger, A. Philip Dawid and Adrian F. M. Smith, 641–649. Oxford:Clarendon Press.
- Greenwood, Jeremy, Zvi Hercowitz, and Gregory W. Huffman.** 1988. “Investment, Capacity Utilization, and the Real Business Cycle.” *American Economic Review*, 78(3): 402–417.
- Jaimovich, Nir, and Sergio Rebelo.** 2009. “Can News about the Future Drive the Business Cycle?” *American Economic Review*, 99(4): 1097–1118.

- Kaplan, Greg, Benjamin Moll, and Giovanni L. Violante.** 2018. “Monetary Policy According to HANK.” *American Economic Review*, 108(3): 697–743.
- King, Robert G., Charles I. Plosser, and Sergio T. Rebelo.** 1988. “Production, Growth and Business Cycles: I. The Basic Neoclassical Model.” *Journal of Monetary Economics*, 21(2): 195 – 232.
- Mertens, Karel, and José Luis Montiel Olea.** 2018. “Marginal Tax Rates and Income: New Time Series Evidence.” *Quarterly Journal of Economics*, 133(4): 1803–1884.
- Piketty, Thomas, and Emmanuel Saez.** 2003. “Income Inequality in the United States, 1913–1998.” *Quarterly Journal of Economics*, 118(1): 1–41.
- Reiter, Michael.** 2009. “Solving Heterogeneous-Agent Models by Projection and Perturbation.” *Journal of Economic Dynamics and Control*, 33(3): 649–665.
- Saez, Emmanuel.** 2004. “Reported Incomes and Marginal Tax Rates, 1960–2000: Evidence and Policy Implications.” *Tax policy and the Economy*, 18: 117–173.
- Schmitt-Grohé, Stephanie, and Martín Uribe.** 2012. “What’s News in Business Cycles.” *Econometrica*, 80(6): 2733–2764.
- U.S. Bureau of Economic Analysis.** 2023a. “Fixed Assets.” Online Data Base. K1TTOTL1ES000: <https://fred.stlouisfed.org/series/K1TTOTL1ES000> (accessed Feb 16, 2023).
- U.S. Bureau of Economic Analysis.** 2023b. “National Income and Product Accounts.” Online Data Base. GPDI: <https://fred.stlouisfed.org/series/GPDI>  
 PCND: <https://fred.stlouisfed.org/series/PCND>  
 PCDG: <https://fred.stlouisfed.org/series/PCDG>  
 PCESV: <https://fred.stlouisfed.org/series/PCESV>  
 GCE: <https://fred.stlouisfed.org/series/GCE>  
 GDPDEF: <https://fred.stlouisfed.org/series/GDPDEF>  
 Tables 1 - 3: <https://apps.bea.gov/iTable/?reqid=19&step=2&isuri=1&categories=survey>  
 (all accessed Feb 16, 2023).
- U.S. Bureau of Labor Statistics.** 2023a. “Current Employment Statistics.” Online Data Base. CNP16OV: <https://fred.stlouisfed.org/series/CNP16OV>  
 (all accessed Feb 16, 2023).
- U.S. Bureau of Labor Statistics.** 2023b. “Productivity and Costs.” Online Data Base. COMPNFB: <https://fred.stlouisfed.org/series/COMPNFB>  
 HOANBS: <https://fred.stlouisfed.org/series/HOANBS>  
 (all accessed Feb 16, 2023).

- U.S. Internal Revenue Service.** 2023. “Statistics of Income.” Online Data Base. <https://www.irs.gov/statistics/soi-tax-stats-historical-data-tables> (accessed Feb 16, 2023).
- U.S. Office of Management and Budget and Federal Reserve Bank of St. Louis.** 2023. “Gross Federal Debt Held by the Public as Percent of Gross Domestic Product.” Online Data Base. FYPUGDA188S: <https://fred.stlouisfed.org/series/FYPUGDA188S> (accessed Feb 16, 2023).
- U.S. Social Security Administration.** 2023. “Annual Statistical Supplement, 2019.” Online Data Base. Table 2.A3: <https://www.ssa.gov/policy/docs/statcomps/supplement/2019/index.html> (accessed Feb 16, 2023).
- World Inequality Database.** 2023. “Top Income and Wealth Shares.” Online Data Base. <https://wid.world/country/usa/> (accessed Feb 16, 2023).
- Wu, Jing Cynthia, and Fan Dora Xia.** 2016. “Measuring the Macroeconomic Impact of Monetary Policy at the Zero Lower Bound.” *Journal of Money, Credit and Banking*, 48(2-3): 253–291.
- Young, Eric R.** 2010. “Solving the Incomplete Markets Model with Aggregate Uncertainty Using the Krusell–Smith Algorithm and Non-Stochastic Simulations.” *Journal of Economic Dynamics and Control*, 34(1): 36–41.